

The Use of Diamond Tiles to Synthesize Modular Phased Arrays

P. Rocca, N. Anselmi, A. Polo, and A. Massa

Contents

1	Numerical Results	3
1.1	OTM - Integer - Hexagon (10,10,10) - Mask Matching - Broadside - $d_{y2} = 0.5\lambda$	3
1.2	OTM - Integer - Hexagon (10,10,10) - Mask Matching - Steering $(\theta, \phi) = (30, 0)$ [deg]	13
1.3	OTM - Integer - Hexagon (10,10,10) - Mask Matching - Steering $(\theta, \phi) = (30, 0)$ [deg] - Markov Init. $N_I = 272$	19
1.4	OTM - Integer - Hexagon (10,10,10) - Mask Matching - Broadside - $d_{y2} = 0.5\lambda$ - Markov Init. $N_I = 542$	28

1 Numerical Results

1.1 OTM - Integer - Hexagon (10,10,10) - Mask Matching - Broadside - $d_{y2} = 0.5\lambda$

Array Geometry

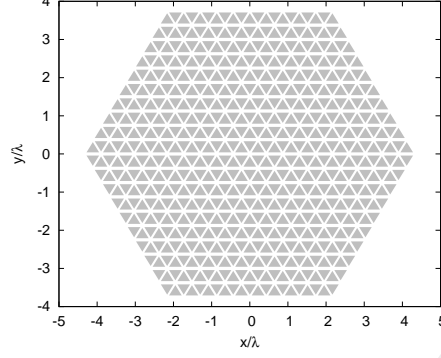


Figure 1: $N_{tot} = 600$, $L_d = 20\lambda$, $d_x = 0.22\lambda$, $d_{y1} = 0.25\lambda$, $d_{y2} = 0.5\lambda$, $N_c^{tot} = 800$, $N_p^{tot} = 441$, $N_p^{(bound)} = 61$, $a = 10$, $b = 10$, $c = 10$ – Array Geometry

Reference Array, Convex Programming Excitations

Test case parameters

- Number of array elements - $N_{tot} = 600$
- Element spacing along x - $d_x = 0.22\lambda$
- Element spacing along y_1 - $d_{y1} = 0.25\lambda$
- Element spacing along y_2 - $d_{y2} = 0.5\lambda$
- Pointing Direction - $\theta_0 = 0^\circ$
- Pointing Direction - $\phi_0 = 0^\circ$
- Pointing Direction - $u_0 = 0$
- Pointing Direction - $v_0 = 0$
- A side length - $a = 10$
- B side length - $b = 10$
- C side length - $c = 10$

Mask Constraints

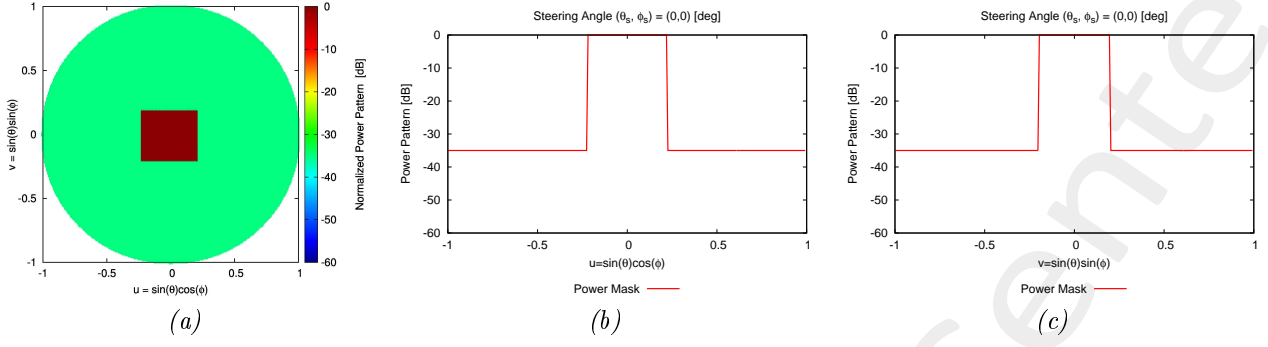


Figure 2: Mask Power Pattern in broadside direction $(\theta, \phi) = (0, 0)$ [deg]: (a) 2D, (b) Normalized cut along azimuth direction, (c) Normalized cut along elevation direction.

Array Tiling

Goal

Applying OTM algorithm with lozenge tiles encoded as integer strings.

Software Parameters

The parameters are:

- Number of array elements - $N_{tot} = 600$
- Element spacing along x - $d_x = 0.22\lambda$
- Element spacing along y_1 - $d_{y1} = 0.25\lambda$
- Element spacing along y_2 - $d_{y2} = 0.5\lambda$
- Side's domain - $L_d = 20\lambda$
- Points number - $N_p^{tot} = 441$
- Points along x - $M_p = 21$
- Points along y - $N_p = 21$
- Total cells number - $N_c^{tot} = 800$
- Cells along x - $M_c = 40$
- Cells along y - $N_c = 20$
- Boundary points - $N_p^{(bound)} = 61$
- Samples along u - $N_u = 256$

- Samples along v - $N_v = 256$
- SLL weight - $w_{SLL} = 0.0$
- Directivity weight - $w_D = 0$
- HPBW weight azimuth - $w_{HPBW}^{azm} = 0.0$
- HPBW weight elevation - $w_{HPBW}^{elv} = 0.0$
- Mask weight - $w_{mask} = 1.0$
- Cell elements - $N_{el} = 1$
- Pointing Direction - $\theta_0 = 0^\circ$
- Pointing Direction - $\phi_0 = 0^\circ$
- Pointing Direction - $u_0 = 0$
- Pointing Direction - $v_0 = 0$
- A side length - $a = 10$
- B side length - $b = 10$
- C side length - $c = 10$
- A side length in λ - $L_a = 4.33\lambda$
- B side length in λ - $L_b = 4.33\lambda$
- C side length in λ - $L_c = 4.33\lambda$
- Tiling configurations - $T = 9.27 \times 10^{33}$
- Number of unknowns - $N_u = 271$
- Maximum of word max - $U_{max} = 10$
- Number of trials (seed) - $N_{seed} = 105$
- Number of individuals - $N_I = 272$
- Number of schemata - $N_{sch} = 56$
- Cross-Over probability - $p_{cx} = 0.9$
- Mutation probability - $p_m = 0.001$
- Diversity Percentage - $d\% = 7\%$

Results

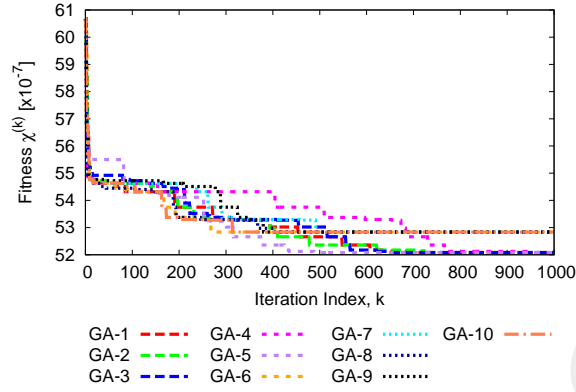


Figure 3: Fitness for 10 best seeds

GA	Seed	SLL [dB]	HPBW (az) [deg]	HPBW (el) [deg]	D [dB]	Fitness Value
1	0.199	-33.52	8.997	8.927	26.773	5.208×10^{-6}
2	0.259	-33.52	8.997	8.927	26.773	5.208×10^{-6}
3	0.378	-33.52	8.997	8.927	26.773	5.208×10^{-6}
4	0.440	-33.52	8.997	8.927	26.773	5.208×10^{-6}
5	0.5	-33.52	8.997	8.927	26.773	5.208×10^{-6}
6	0.024	-33.59	8.998	8.929	26.772	5.283×10^{-6}
7	0.0	-33.59	8.998	8.929	26.772	5.283×10^{-6}
8	0.152	-33.59	8.998	8.929	26.772	5.283×10^{-6}
9	0.222	-33.59	8.998	8.929	26.772	5.283×10^{-6}
10	0.225	-33.59	8.998	8.929	26.772	5.283×10^{-6}

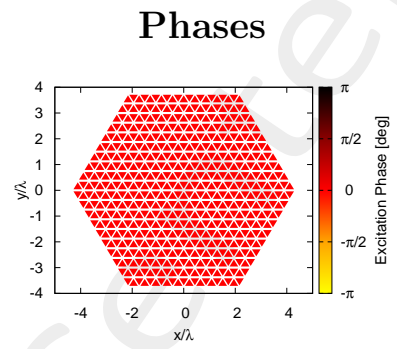
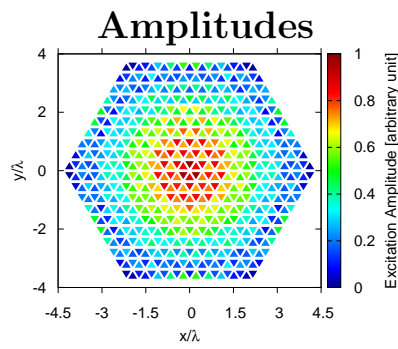
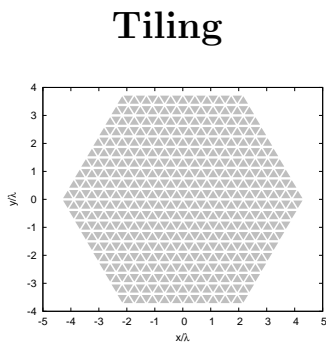
Table 3: Solution Parameters of Radiation Pattern along $(\theta_0, \phi_0) = (0, 0)$ [deg]

Fig. 3 represents the fitness value for 10 best seeds.

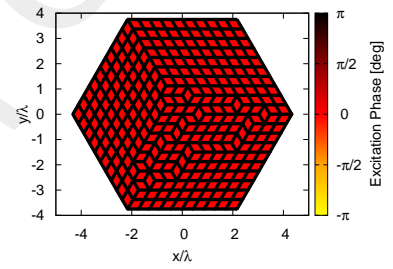
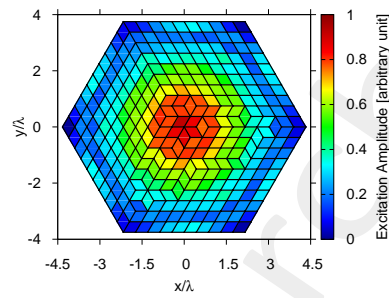
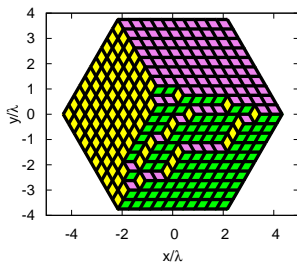
I analyzed the solution (seed) that permits to reach the minimum fitness value. The solutions analyzed corresponds to $seed = \{0.199; 0.259; 0.378; 0.440; 0.5\}$.

Broadside Analysis

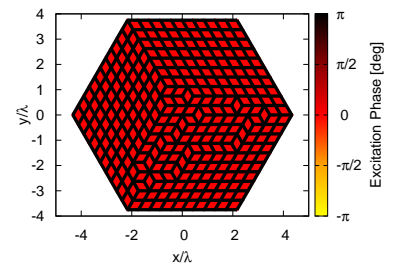
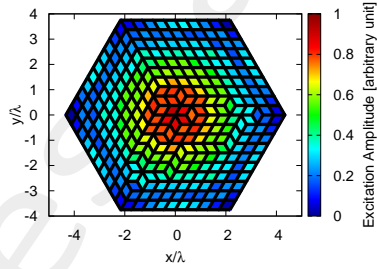
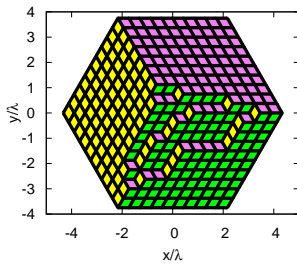
Reference



Seed : 0.199



Seed : 0.259



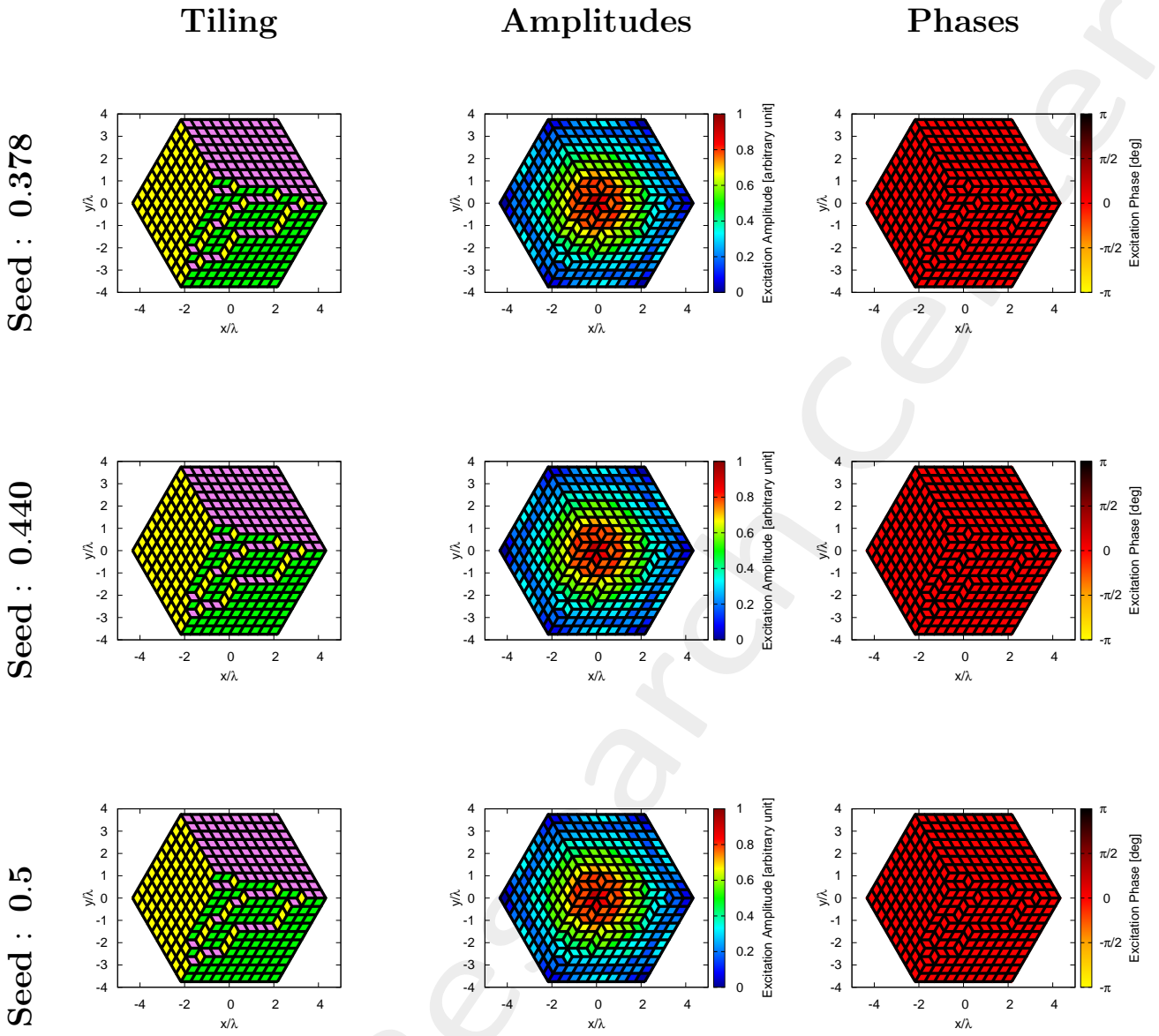


Figure 4: *Mask Matching*, $SLL = -34.79 [dB]$, $N_{tot} = 600$, $L_d = 20\lambda$, $d_x = 0.22\lambda$, $d_{y1} = 0.25\lambda$, $d_{y2} = 0.5\lambda$, $a = 10$, $b = 10$, $c = 10$, $(\theta_0, \phi_0) = (0, 0) [deg]$ – Solution ID.: Reference, Seed 0.199, Seed 0.259, Seed 0.378, Seed 0.440, Seed 0.5

The best solutions have the same tiling configuration, so the radiation properties are the same, so I analyze only the first solution with $seed = \{0.199\}$.

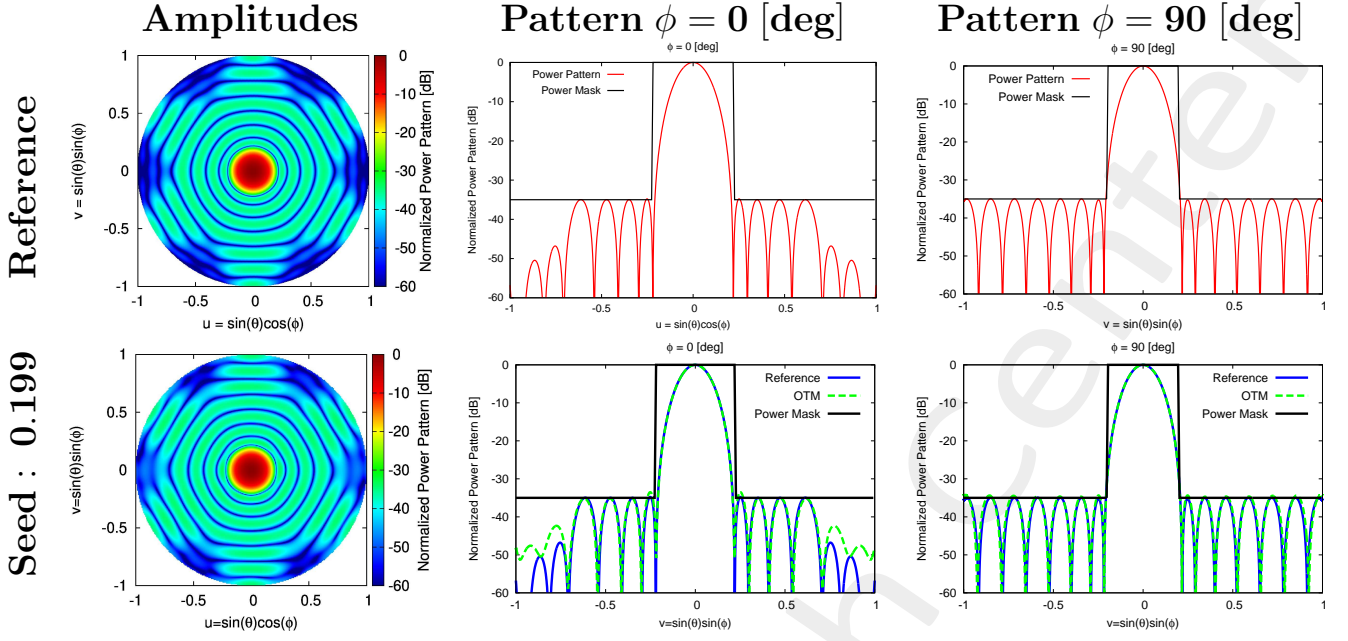


Figure 5: *Mask Matching*, $SLL = -34.79$ [dB], $N_{tot} = 600$, $L_d = 20\lambda$, $d_x = 0.22\lambda$, $d_{y1} = 0.25\lambda$, $d_{y2} = 0.5\lambda$, $a = 10$, $b = 10$, $c = 10$, $(\theta_0, \phi_0) = (0, 0)$ [deg] – Solution ID.: Reference, Seed 0.199

Steering Analysis

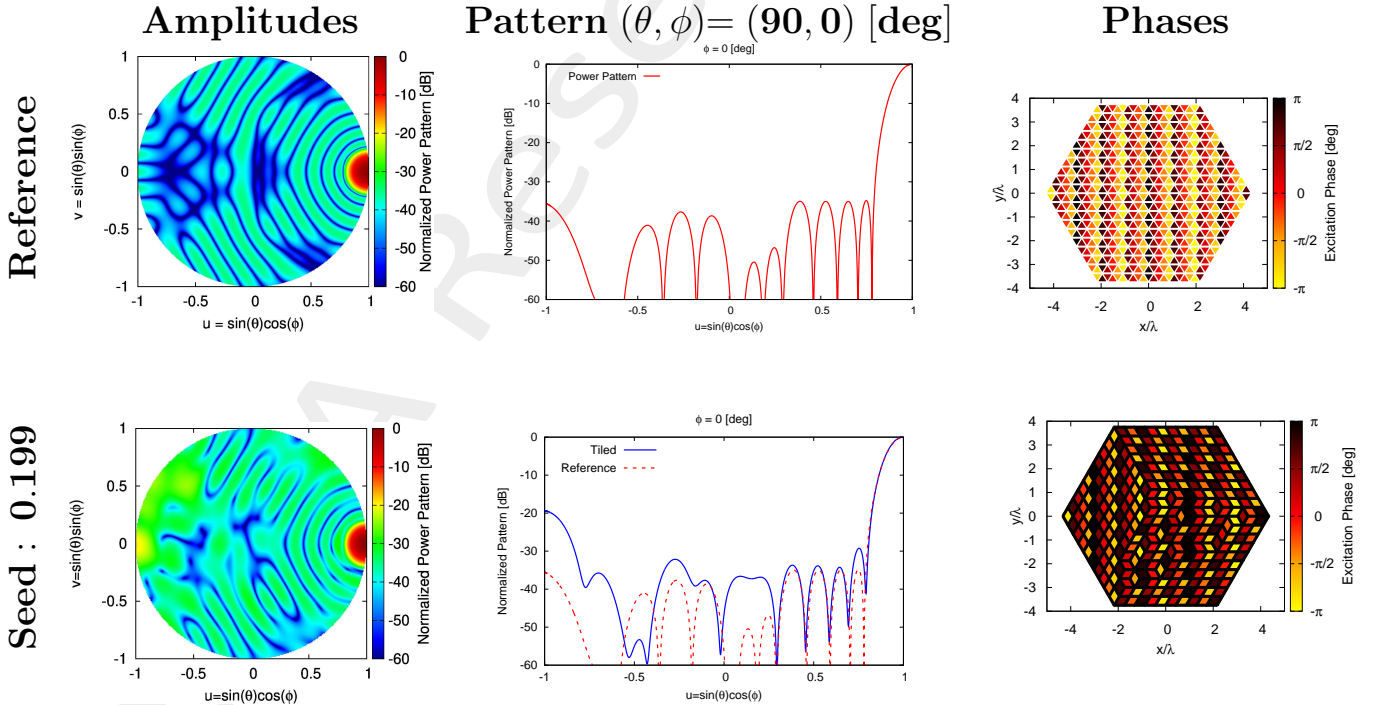


Figure 6: *Mask Matching*, $SLL = -34.79$ [dB], $N_{tot} = 600$, $L_d = 20\lambda$, $d_x = 0.22\lambda$, $d_{y1} = 0.25\lambda$, $d_{y2} = 0.5\lambda$, $a = 10$, $b = 10$, $c = 10$, $(\theta_0, \phi_0) = (90, 0)$ [deg] – Solution ID.: Reference, Seed 0.199

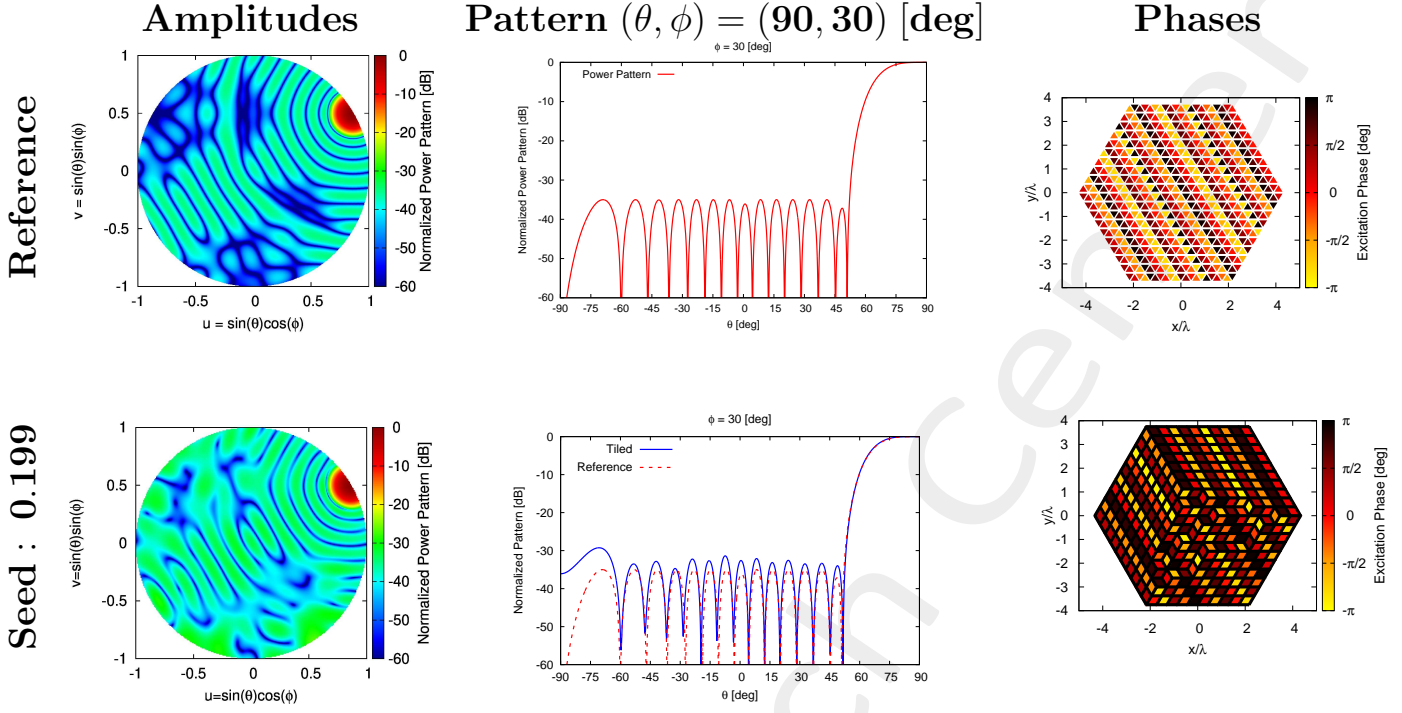


Figure 7: Mask Matching, $SLL = -34.79$ [dB], $N_{tot} = 600$, $L_d = 20\lambda$, $d_x = 0.22\lambda$, $d_{y1} = 0.25\lambda$, $d_{y2} = 0.5\lambda$, $a = 10$, $b = 10$, $c = 10$, $(\theta_0, \phi_0) = (90, 30)$ [deg] – Solution ID.: Reference, Seed 0.199

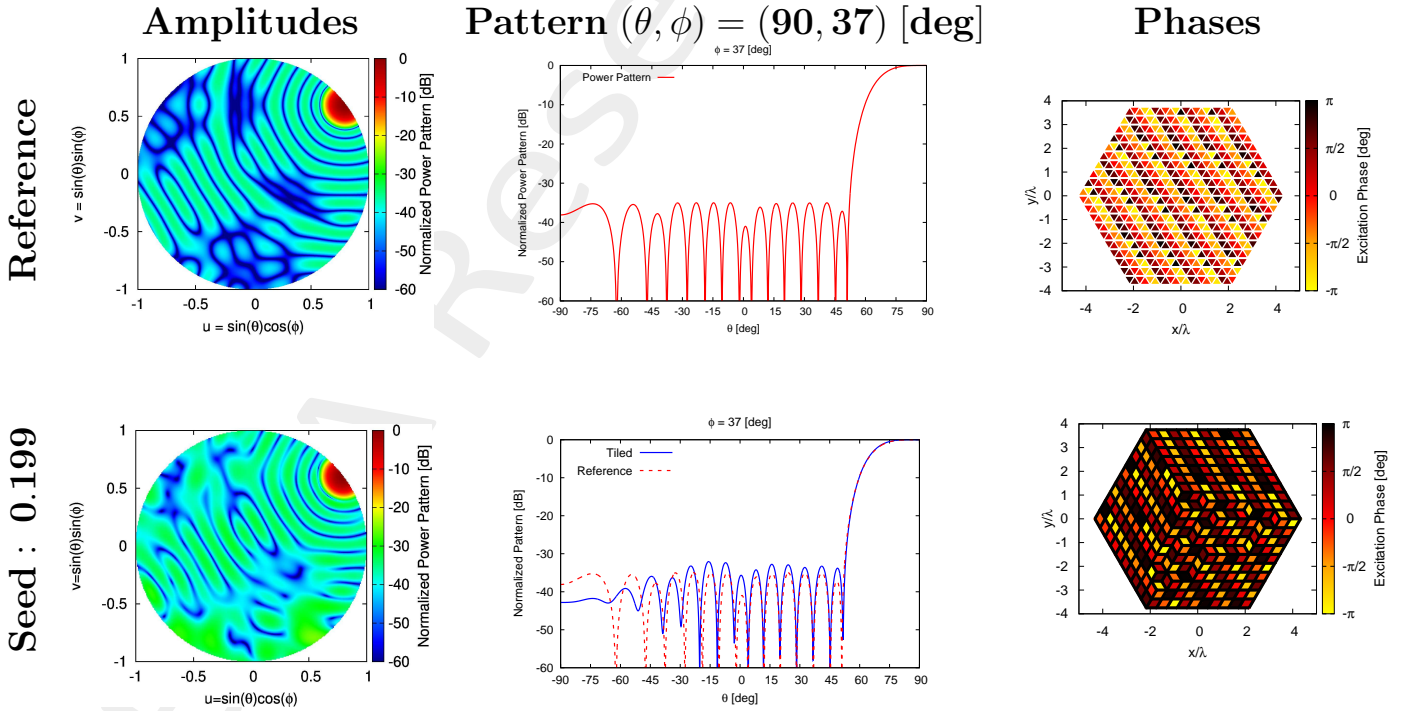


Figure 8: Mask Matching, $SLL = -34.79$ [dB], $N_{tot} = 600$, $L_d = 20\lambda$, $d_x = 0.22\lambda$, $d_{y1} = 0.25\lambda$, $d_{y2} = 0.5\lambda$, $a = 10$, $b = 10$, $c = 10$, $(\theta_0, \phi_0) = (90, 37)$ [deg] – Solution ID.: Reference, Seed 0.199

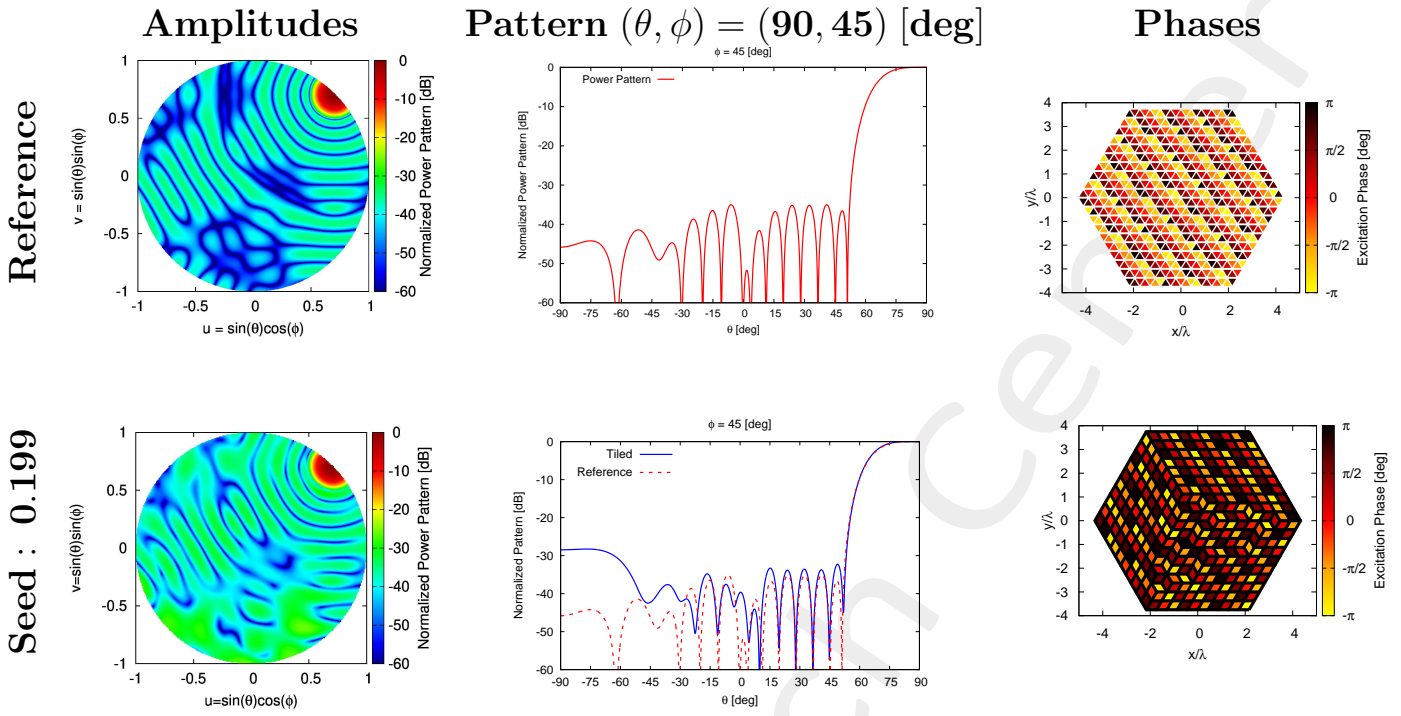


Figure 9: *Mask Matching*, $SLL = -34.79$ [dB], $N_{tot} = 600$, $L_d = 20\lambda$, $d_x = 0.22\lambda$, $d_{y1} = 0.25\lambda$, $d_{y2} = 0.5\lambda$, $a = 10$, $b = 10$, $c = 10$, $(\theta_0, \phi_0) = (90, 45)$ [deg] – Solution ID.: Reference, Seed 0.199

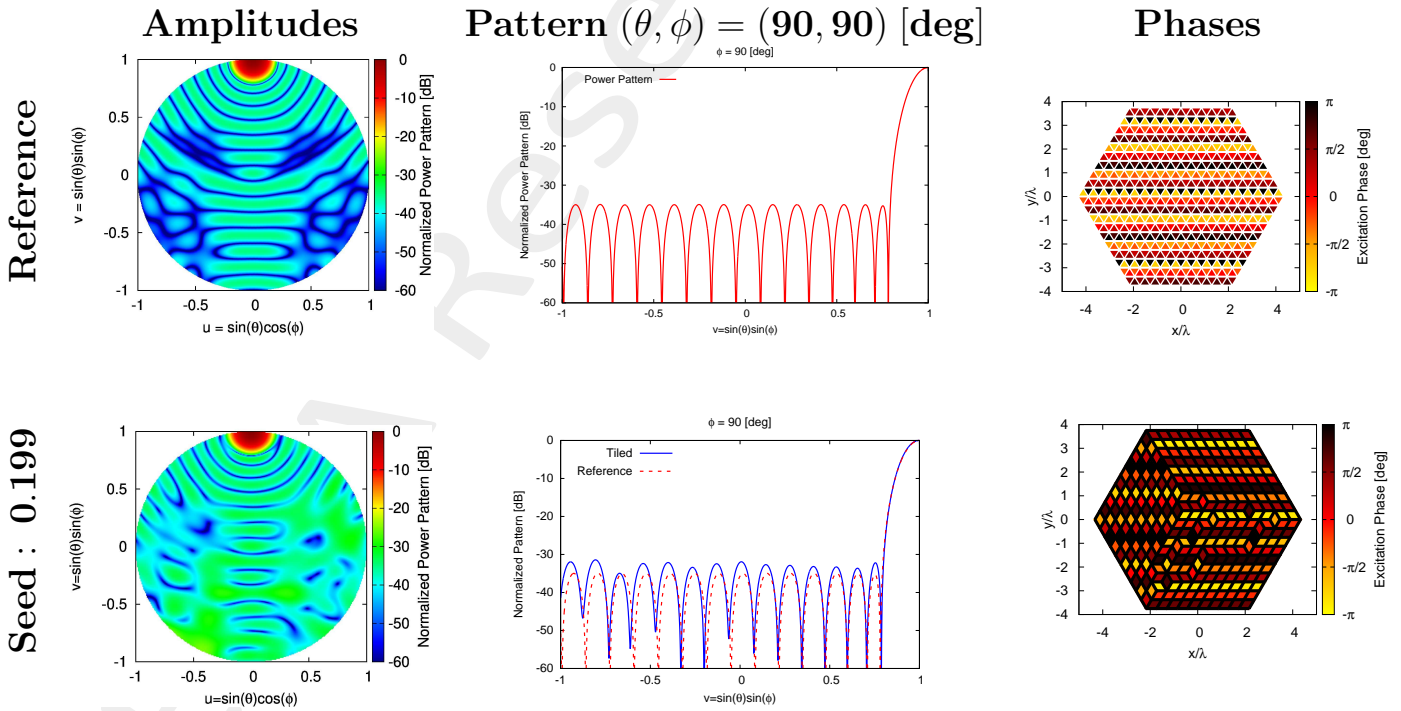


Figure 10: *Mask Matching*, $SLL = -34.79$ [dB], $N_{tot} = 600$, $L_d = 20\lambda$, $d_x = 0.22\lambda$, $d_{y1} = 0.25\lambda$, $d_{y2} = 0.5\lambda$, $a = 10$, $b = 10$, $c = 10$, $(\theta_0, \phi_0) = (90, 90)$ [deg] – Solution ID.: Reference, Seed 0.199

Solutions Summary

(a, b, c)	MAX_ITE (# iterations)	$\Delta\tau$ [sec] (single simulation period)	τ [sec] total simulation period
10, 10, 10	1000	0.050148	50.148

Table 12: Simulation Time

SOLUTION ID	SLL [dB]	HPBW (azimuth) [deg]	HPBW (elevation) [deg]	D [dB]	Mask Fitting
Reference	-34.788	9.003	8.914	26.791	0
Seed 0.199	-33.52	8.997	8.927	26.773	5.208×10^{-6}
Seed 0.259	-33.52	8.997	8.927	26.773	5.208×10^{-6}
Seed 0.378	-33.52	8.997	8.927	26.773	5.208×10^{-6}
Seed 0.440	-33.52	8.997	8.927	26.773	5.208×10^{-6}
Seed 0.5	-33.52	8.997	8.927	26.773	5.208×10^{-6}

Table 13: SLL, $HPBW_{az}$, $HPBW_{el}$, D, Mask Fitting of Radiation Pattern along $(\theta_0, \phi_0) = (0, 0)$ [deg]

1.2 OTM - Integer - Hexagon (10,10,10) - Mask Matching - Steering $(\theta, \phi) = (30, 0)$ [deg]

Array Geometry

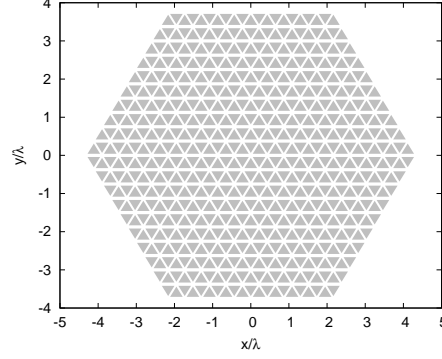


Figure 11: $N_{tot} = 600$, $L_d = 20\lambda$, $d_x = 0.22\lambda$, $d_{y1} = 0.25\lambda$, $d_{y2} = 0.5\lambda$, $N_c^{tot} = 800$, $N_p^{tot} = 441$, $N_p^{(bound)} = 61$, $a = 10$, $b = 10$, $c = 10$ – Array Geometry

Reference Array, Convex Programming Excitations

Test case parameters

The parameters are:

- Number of array elements - $N_{tot} = 600$
- Element spacing along x - $d_x = 0.22\lambda$
- Element spacing along y_1 - $d_{y1} = 0.25\lambda$
- Element spacing along y_2 - $d_{y2} = 0.5\lambda$
- Pointing Direction - $\theta_0 = 30^\circ$
- Pointing Direction - $\phi_0 = 0^\circ$
- Pointing Direction - $u_0 = 0.5$
- Pointing Direction - $v_0 = 0$
- A side length - $a = 10$
- B side length - $b = 10$
- C side length - $c = 10$

Mask Constraints

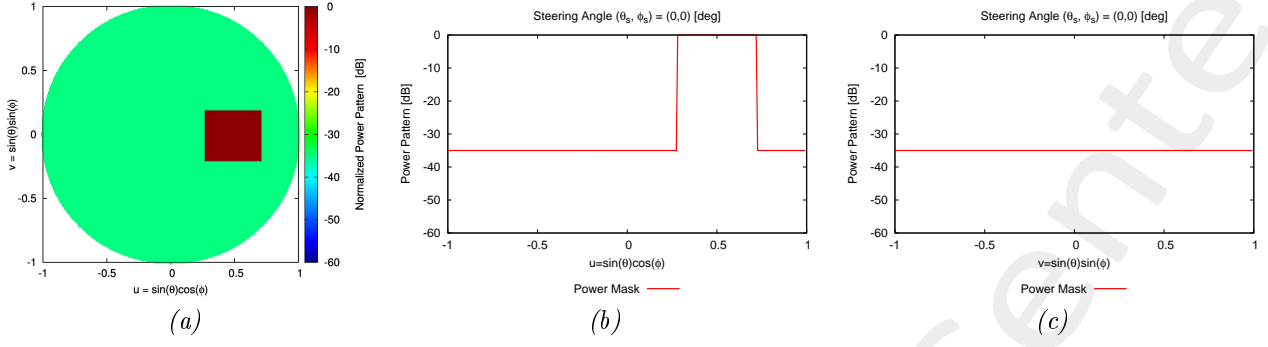


Figure 12: Mask Power Pattern in broadside direction $(\theta, \phi) = (30, 0)$ [deg]: (a) 2D, (b) Normalized cut along azimuth direction, (c) Normalized cut along elevation direction.

Array Tiling

Goal

Applying OTM algorithm with lozenge tiles encoded as integer strings.

Software Parameters

- Number of array elements - $N_{tot} = 600$
- Element spacing along x - $d_x = 0.22\lambda$
- Element spacing along y_1 - $d_{y1} = 0.25\lambda$
- Element spacing along y_2 - $d_{y2} = 0.5\lambda$
- Side's domain - $L_d = 20\lambda$
- Points number - $N_p^{tot} = 441$
- Points along x - $M_p = 21$
- Points along y - $N_p = 21$
- Total cells number - $N_c^{tot} = 800$
- Cells along x - $M_c = 40$
- Cells along y - $N_c = 20$
- Boundary points - $N_p^{(bound)} = 61$
- Samples along u - $N_u = 256$
- Samples along v - $N_v = 256$

- SLL weight - $w_{SLL} = 0.0$
- Directivity weight - $w_D = 0$
- HPBW weight azimuth - $w_{HPBW}^{azm} = 0.0$
- HPBW weight elevation - $w_{HPBW}^{elv} = 0.0$
- Mask weight - $w_{mask} = 1.0$
- Cell elements - $N_{el} = 1$
- Pointing Direction - $\theta_0 = 30^\circ$
- Pointing Direction - $\phi_0 = 0^\circ$
- Pointing Direction - $u_0 = 0.5$
- Pointing Direction - $v_0 = 0$
- A side length - $a = 10$
- B side length - $b = 10$
- C side length - $c = 10$
- A side length in λ - $L_a = 4.33\lambda$
- B side length in λ - $L_b = 4.33\lambda$
- C side length in λ - $L_c = 4.33\lambda$
- Tiling configurations - $T = 9.27 \times 10^{33}$
- Number of unknowns - $N_u = 271$
- Maximum of word max - $U_{max} = 10$
- Number of trials (seed) - $N_{seed} = 105$
- Number of individuals - $N_I = 272$
- Number of schemata - $N_{sch} = 56$
- Cross-Over probability - $p_{cx} = 0.9$
- Mutation probability - $p_m = 0.001$
- Diversity Percentage - $d\% = 7\%$

Results

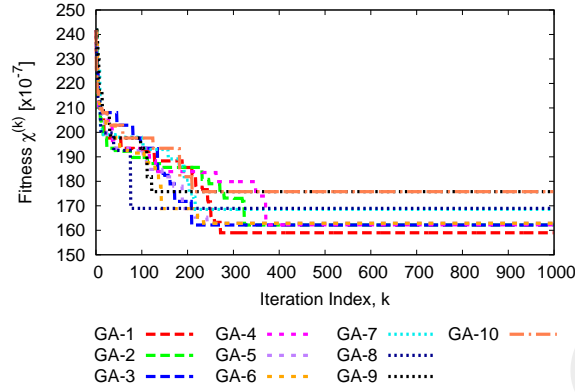


Figure 13: Fitness for 10 best seeds

GA	Seed	SLL [dB]	HPBW (az) [deg]	HPBW (el) [deg]	D [dB]	Fitness Value
1	0.25	-33.542	8.995	8.927	26.774	1.589×10^{-5}
2	0.126	-33.383	8.993	8.923	26.777	1.621×10^{-5}
3	0.846	-33.383	8.993	8.923	26.777	1.621×10^{-5}
4	0.222	-33.527	8.995	8.926	26.775	1.622×10^{-5}
5	0.067	-33.531	8.995	8.927	26.775	1.629×10^{-5}
6	0.231	-33.531	8.995	8.927	26.775	1.629×10^{-5}
7	0.326	-33.371	8.993	8.923	26.777	1.685×10^{-5}
8	0.087	-33.712	8.996	8.929	26.773	1.689×10^{-5}
9	0.551	-33.423	8.994	8.923	26.776	1.758×10^{-5}
10	0.724	-33.423	8.994	8.923	26.776	1.758×10^{-5}

Table 16: Solution Parameters of Radiation Pattern along $(\theta_0, \phi_0) = (30, 0)$ [deg]

Fig. 13 represents the fitness value for 10 best seeds.

I analyzed the solution (seed) that permits to reach the minimum fitness value. The fitness analyzed corresponds to $seed = \{0.25\}$.

Broadside Analysis

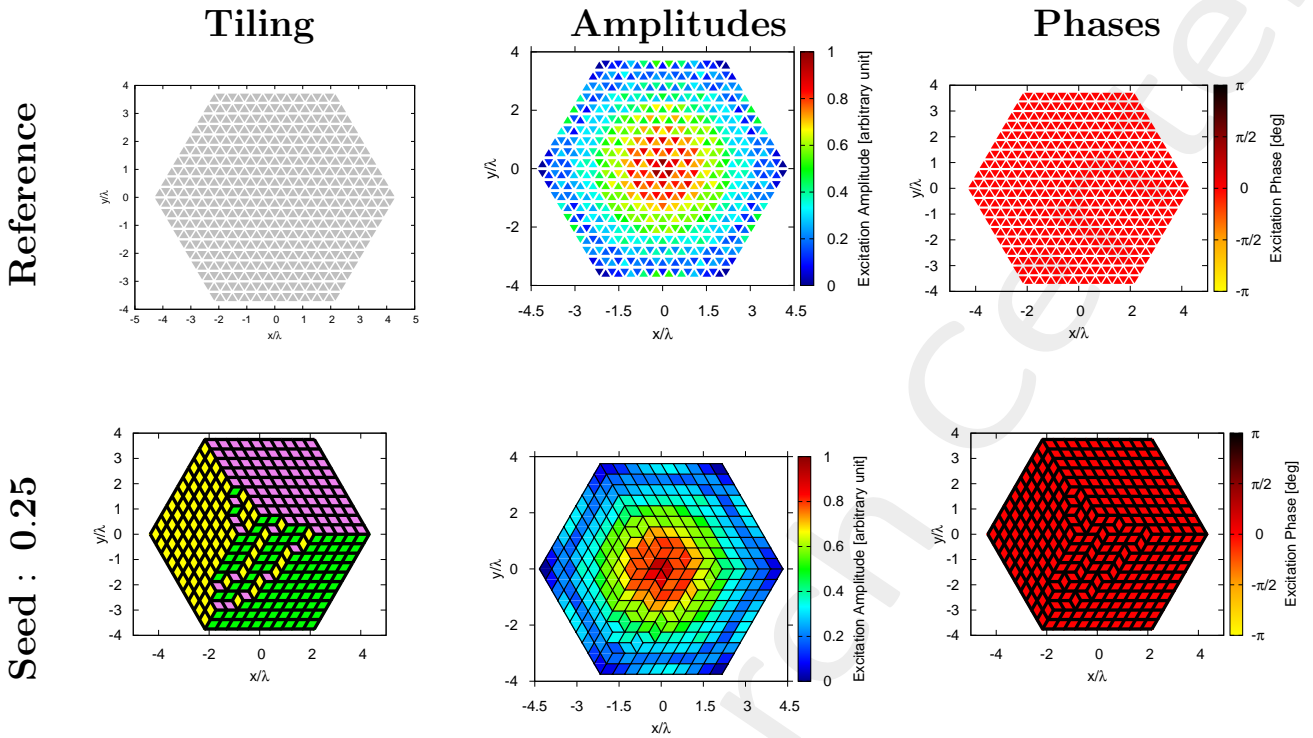


Figure 14: *Mask Matching*, $SLL = -34.79$ [dB], $N_{tot} = 600$, $L_d = 20\lambda$, $d_x = 0.22\lambda$, $d_{y1} = 0.25\lambda$, $d_{y2} = 0.5\lambda$, $a = 10$, $b = 10$, $c = 10$, $(\theta_0, \phi_0) = (0, 0)$ [deg] – Solution ID.: Reference, Seed 0.25

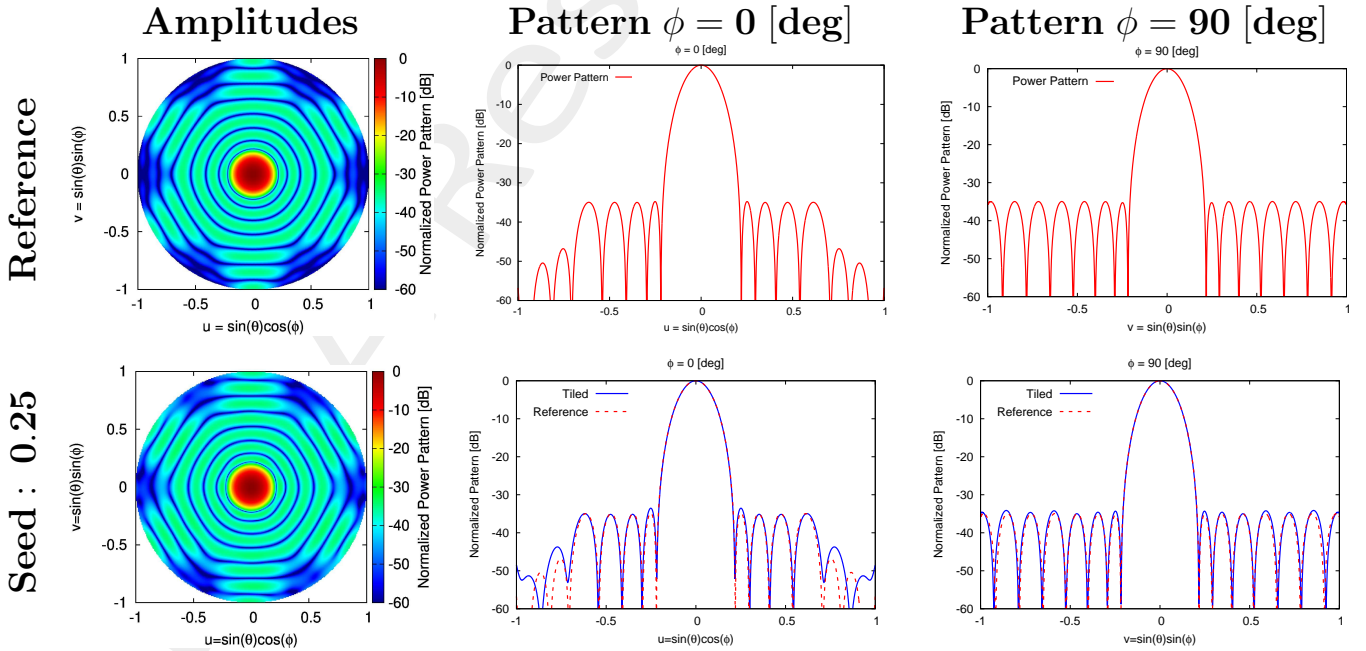


Figure 15: *Mask Matching*, $SLL = -34.79$ [dB], $N_{tot} = 600$, $L_d = 20\lambda$, $d_x = 0.22\lambda$, $d_{y1} = 0.25\lambda$, $d_{y2} = 0.5\lambda$, $a = 10$, $b = 10$, $c = 10$, $(\theta_0, \phi_0) = (0, 0)$ [deg] – Solution ID.: Reference, Seed 0.25

Steering Analysis

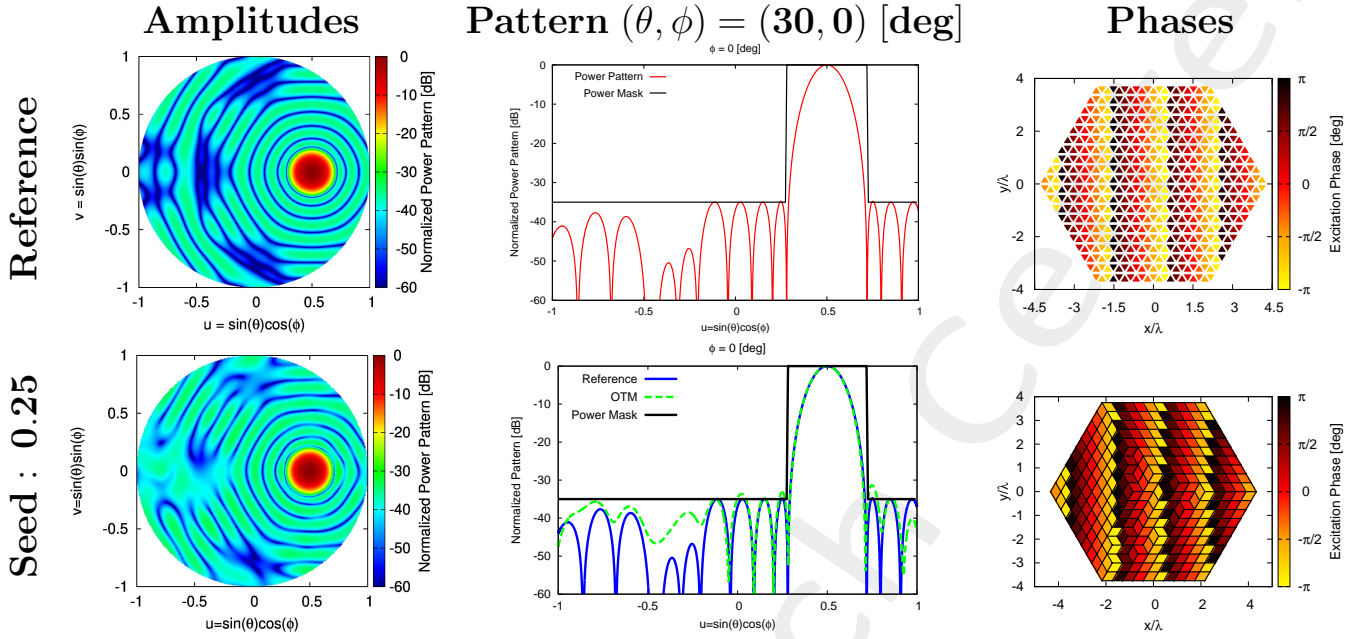


Figure 16: *Mask Matching*, $SLL = -34.79$ [dB], $N_{tot} = 600$, $L_d = 20\lambda$, $d_x = 0.22\lambda$, $d_{y1} = 0.25\lambda$, $d_{y2} = 0.5\lambda$, $a = 10$, $b = 10$, $c = 10$, $(\theta_0, \phi_0) = (30, 0)$ [deg] – Solution ID.: Reference, Seed 0.25

Solutions Summary

(a, b, c)	MAX_ITE (# iterations)	$\Delta\tau$ [sec] (single simulation period)	τ [sec] total simulation period
10, 10, 10	1000	0.038459	38.459

Table 20: Simulation Time

SOLUTION ID	SLL [dB]	HPBW (azimuth) [deg]	HPBW (elevation) [deg]	D [dB]	Mask Fitting
Reference	-34.788	10.415	8.914	26.132	0
Seed 0.25	-33.542	8.995	8.927	26.774	1.589×10^{-5}

Table 21: SLL , $HPBW_{az}$, $HPBW_{el}$, D , *Mask Fitting of Radiation Pattern* along $(\theta_0, \phi_0) = (30, 0)$ [deg]

Conclusion

The solution with OTM-GA [Sec. 1.2] is a good choice respect to ETM for the same array architecture; because it is possible to obtain good results with less computational effort.

1.3 OTM - Integer - Hexagon (10,10,10) - Mask Matching - Steering $(\theta, \phi) = (30, 0)$ [deg] - Markov Init. $N_I = 272$

Array Geometry

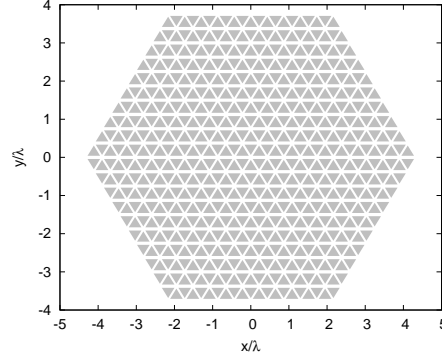


Figure 17: $N_{tot} = 600$, $L_d = 20\lambda$, $d_x = 0.22\lambda$, $d_{y1} = 0.25\lambda$, $d_{y2} = 0.5\lambda$, $N_c^{tot} = 800$, $N_p^{tot} = 441$, $N_p^{(bound)} = 61$, $a = 10$, $b = 10$, $c = 10$ – Array Geometry

Reference Array, Convex Programming Excitations

Test case parameters

- Number of array elements - $N_{tot} = 600$
- Element spacing along x - $d_x = 0.22\lambda$
- Element spacing along y_1 - $d_{y1} = 0.25\lambda$
- Element spacing along y_2 - $d_{y2} = 0.5\lambda$
- Pointing Direction - $\theta_0 = 30^\circ$
- Pointing Direction - $\phi_0 = 0^\circ$
- Pointing Direction - $u_0 = 0.5$
- Pointing Direction - $v_0 = 0$
- A side length - $a = 10$
- B side length - $b = 10$
- C side length - $c = 10$

Mask Constraints

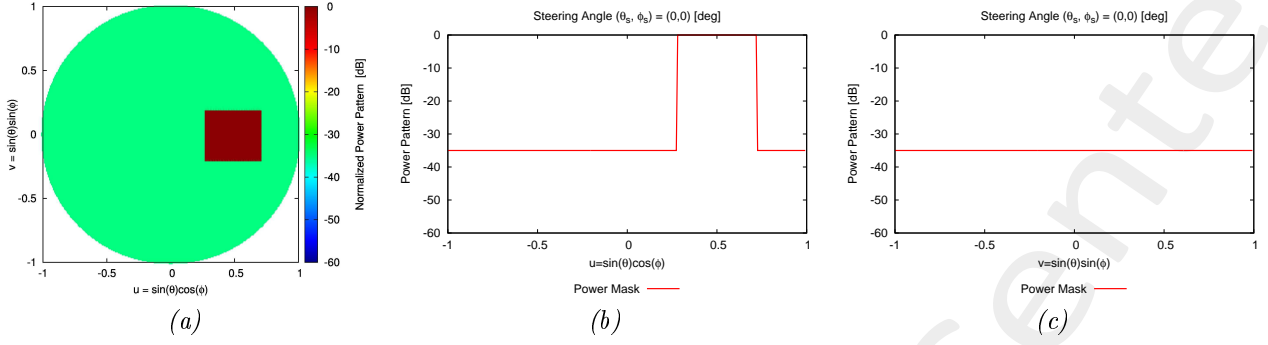


Figure 18: Mask Power Pattern in broadside direction $(\theta, \phi) = (30, 0)$ [deg]: (a) 2D, (b) Normalized cut along azimuth direction, (c) Normalized cut along elevation direction.

Array Tiling

Goal

Applying OTM algorithm with lozenge tiles encoded as integer strings.

Software Parameters

The parameters are:

- Number of array elements - $N_{tot} = 600$
- Element spacing along x - $d_x = 0.22\lambda$
- Element spacing along y_1 - $d_{y1} = 0.25\lambda$
- Element spacing along y_2 - $d_{y2} = 0.5\lambda$
- Side's domain - $L_d = 20\lambda$
- Points number - $N_p^{tot} = 441$
- Points along x - $M_p = 21$
- Points along y - $N_p = 21$
- Total cells number - $N_c^{tot} = 800$
- Cells along x - $M_c = 40$
- Cells along y - $N_c = 20$
- Boundary points - $N_p^{(bound)} = 61$
- Samples along u - $N_u = 256$

- Samples along v - $N_v = 256$
- SLL weight - $w_{SLL} = 0.0$
- Directivity weight - $w_D = 0$
- HPBW weight azimuth - $w_{HPBW}^{azm} = 0.0$
- HPBW weight elevation - $w_{HPBW}^{elv} = 0.0$
- Mask weight - $w_{mask} = 1.0$
- Cell elements - $N_{el} = 1$
- Pointing Direction - $\theta_0 = 30^\circ$
- Pointing Direction - $\phi_0 = 0^\circ$
- Pointing Direction - $u_0 = 0.5$
- Pointing Direction - $v_0 = 0$
- A side length - $a = 10$
- B side length - $b = 10$
- C side length - $c = 10$
- A side length in λ - $L_a = 4.33\lambda$
- B side length in λ - $L_b = 4.33\lambda$
- C side length in λ - $L_c = 4.33\lambda$
- Tiling configurations - $T = 9.27 \times 10^{33}$
- Number of unknowns - $N_u = 271$
- Maximum of word max - $U_{max} = 10$
- Number of trials (seed) - $N_{seed} = 105$
- Number of individuals - $N_I = 272$
- Number of flips - $N_{flips} = 200$
- Cross-Over probability - $p_{cx} = 0.9$
- Mutation probability - $p_m = 0.001$

Results

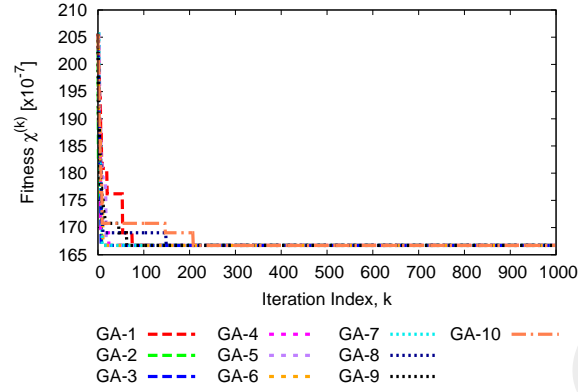


Figure 19: Fitness for 10 best seeds

GA	Seed	SLL [dB]	HPBW (az) [deg]	HPBW (el) [deg]	D [dB]	Fitness Value
1	0.0	-33.739	8.997	8.929	26.773	1.667×10^{-5}
2	0.15	-33.739	8.997	8.929	26.773	1.667×10^{-5}
3	0.205	-33.739	8.997	8.929	26.773	1.667×10^{-5}
4	0.222	-33.739	8.997	8.929	26.773	1.667×10^{-5}
5	0.283	-33.739	8.997	8.929	26.773	1.667×10^{-5}
6	0.440	-33.739	8.997	8.929	26.773	1.667×10^{-5}
7	0.441	-33.739	8.997	8.929	26.773	1.667×10^{-5}
8	0.45	-33.739	8.997	8.929	26.773	1.667×10^{-5}
9	0.597	-33.739	8.997	8.929	26.773	1.667×10^{-5}
10	0.649	-33.739	8.997	8.929	26.773	1.667×10^{-5}

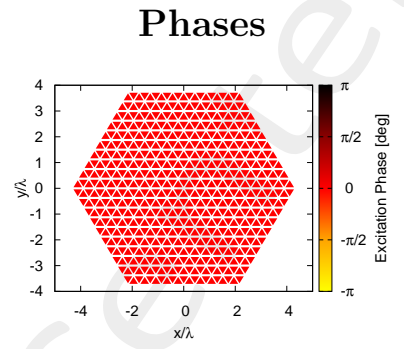
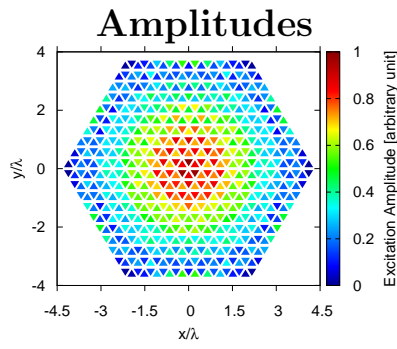
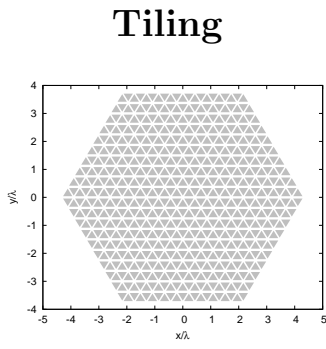
Table 24: Solution Parameters of Radiation Pattern along $(\theta_0, \phi_0) = (30, 0)$ [deg]

Fig. 19 represents the fitness value for 10 best seeds.

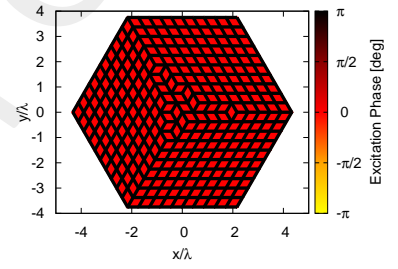
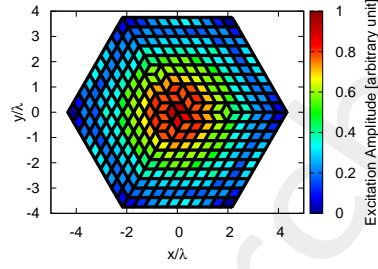
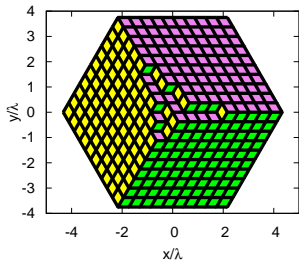
I analyzed the solution (seed) that permits to reach the minimum fitness value. The fitness analyzed corresponds to all seed indicate in the table.

Broadside Analysis

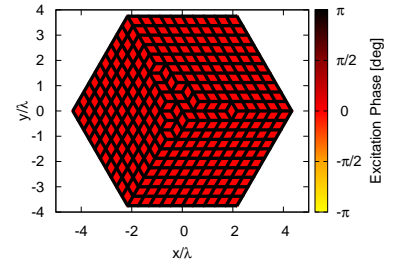
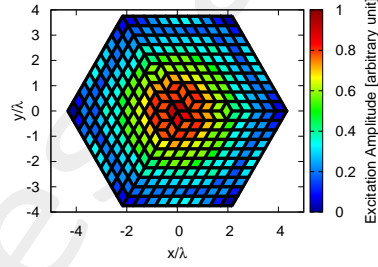
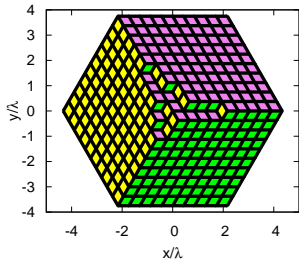
Reference



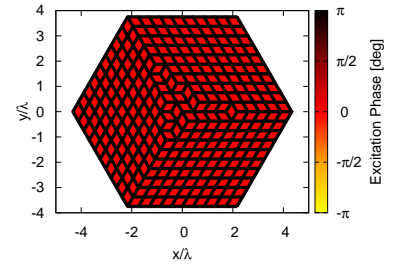
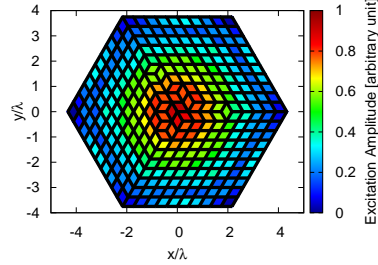
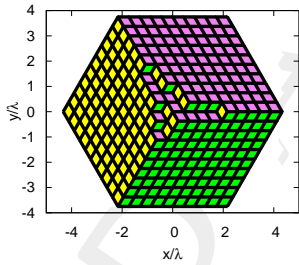
Seed : 0.0



Seed : 0.15



Seed : 0.205

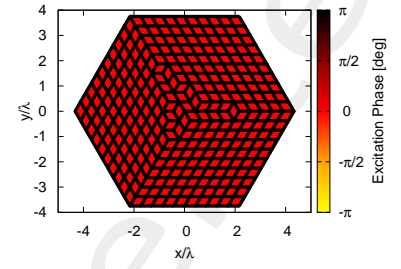
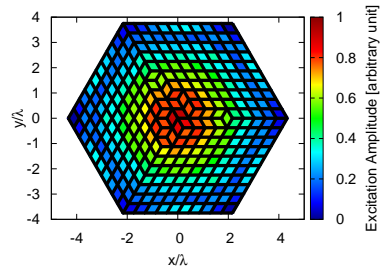
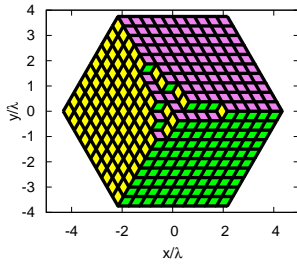


Tiling

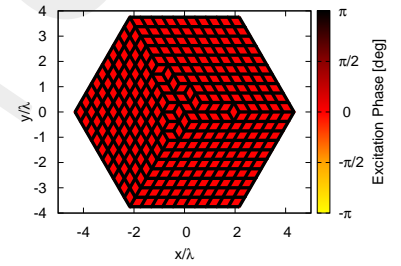
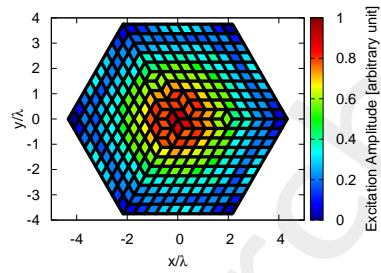
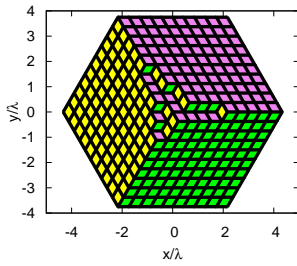
Amplitudes

Phases

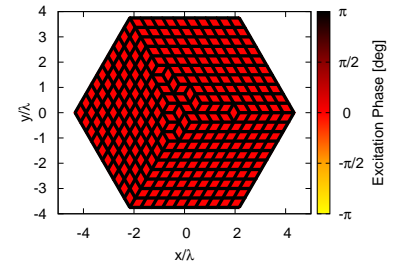
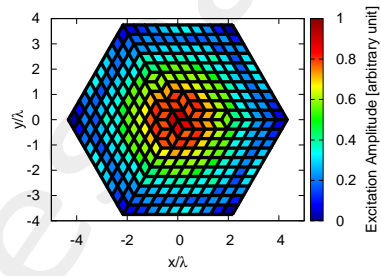
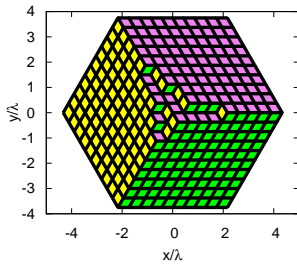
Seed : 0.222



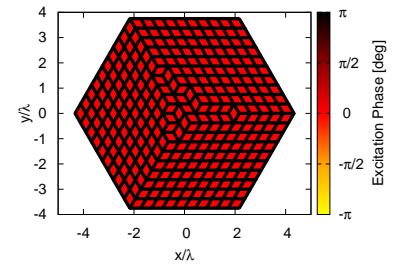
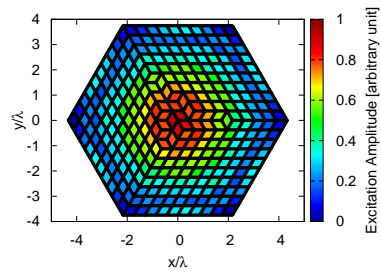
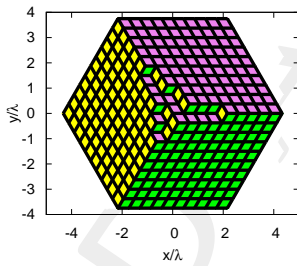
Seed : 0.283



Seed : 0.440



Seed : 0.441



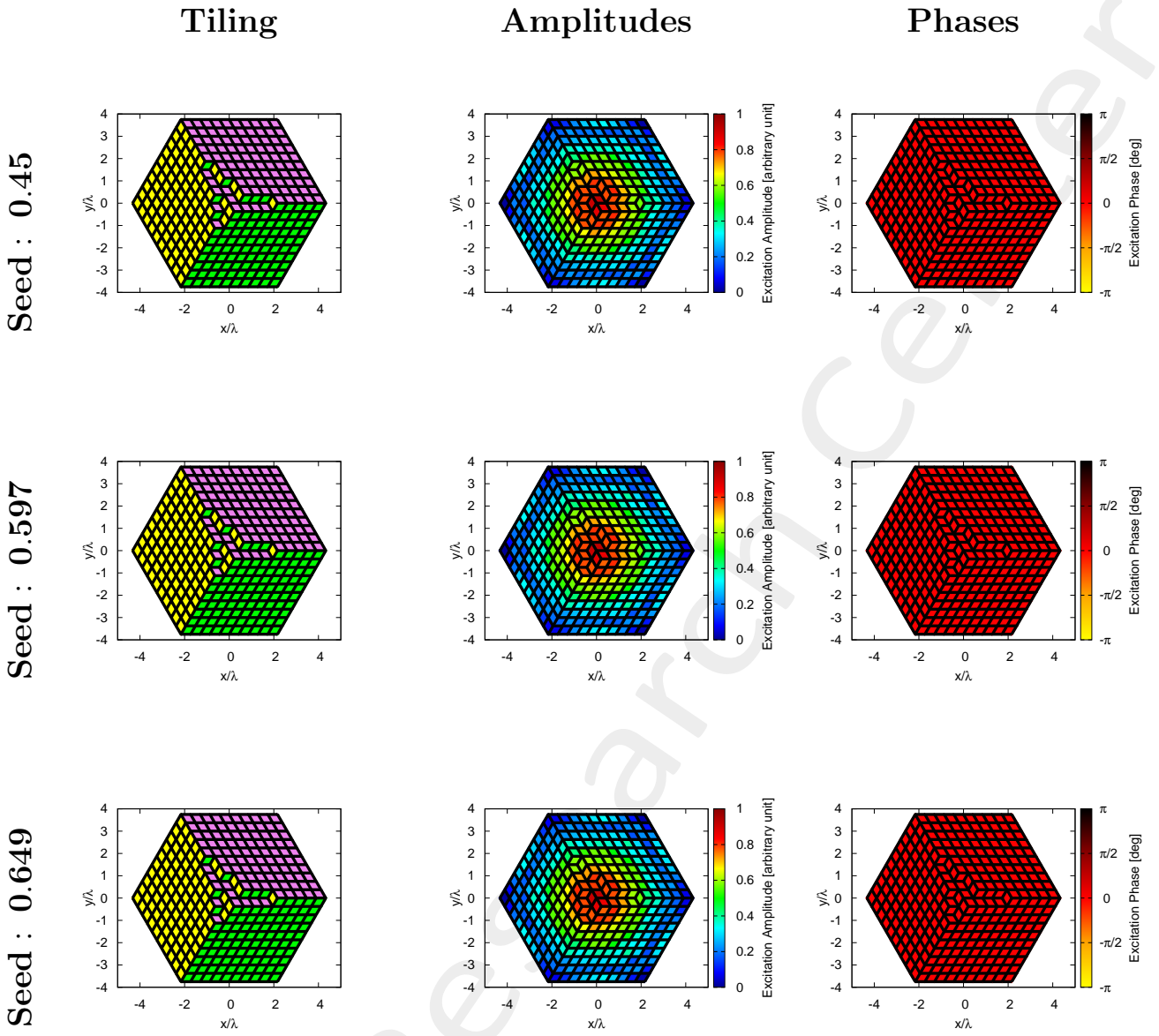


Figure 20: *Mask Matching*, $SLL = -34.79$ [dB], $N_{tot} = 600$, $L_d = 20\lambda$, $d_x = 0.22\lambda$, $d_{y1} = 0.25\lambda$, $d_{y2} = 0.5\lambda$, $a = 10$, $b = 10$, $c = 10$, $(\theta_0, \phi_0) = (0, 0)$ [deg] – Solution ID.: Reference, Seed 0.0, Seed 0.15, Seed 0.205, Seed 0.222, Seed 0.283, Seed 0.440, Seed 0.441, Seed 0.45, Seed 0.597, Seed 0.649

The best solutions have the same tiling configuration, so the radiation properties are the same, so I analyze only the first solution with $seed = \{0.0\}$.

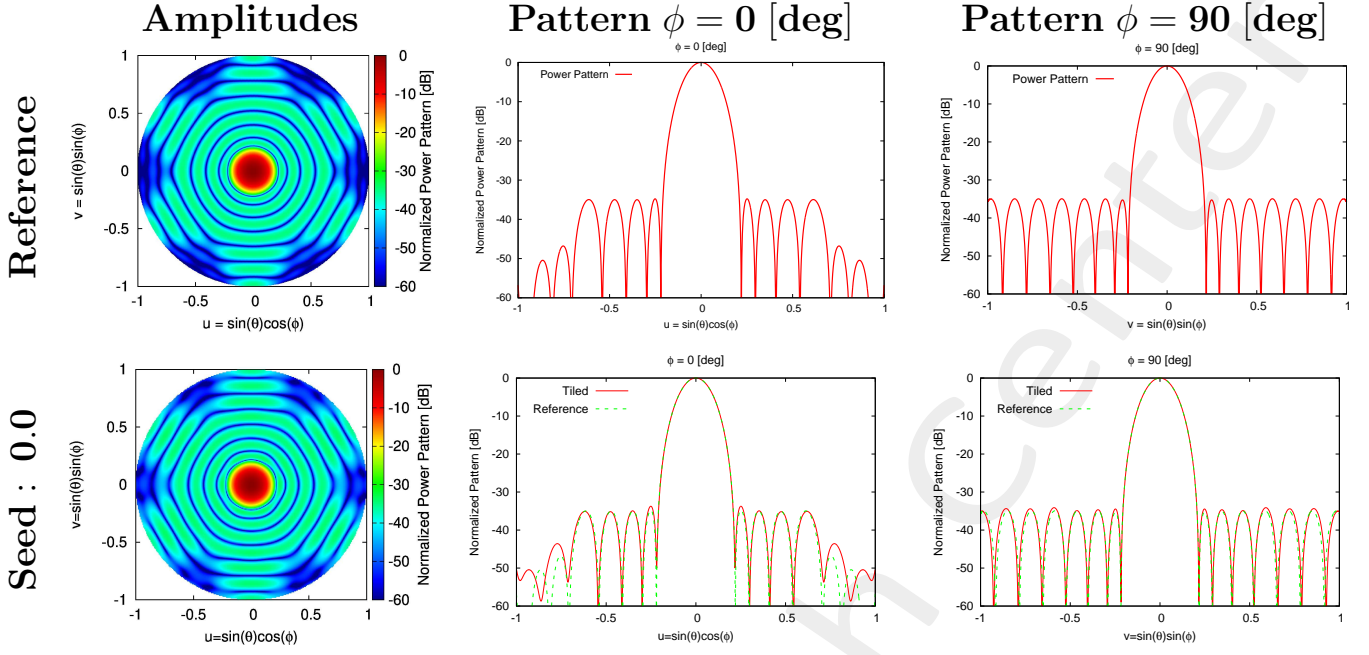


Figure 21: *Mask Matching*, $SLL = -34.79$ [dB], $N_{tot} = 600$, $L_d = 20\lambda$, $d_x = 0.22\lambda$, $d_{y1} = 0.25\lambda$, $d_{y2} = 0.5\lambda$, $a = 10$, $b = 10$, $c = 10$, $(\theta_0, \phi_0) = (0, 0)$ [deg] – Solution ID.: Reference, Seed 0.0

Steering Analysis

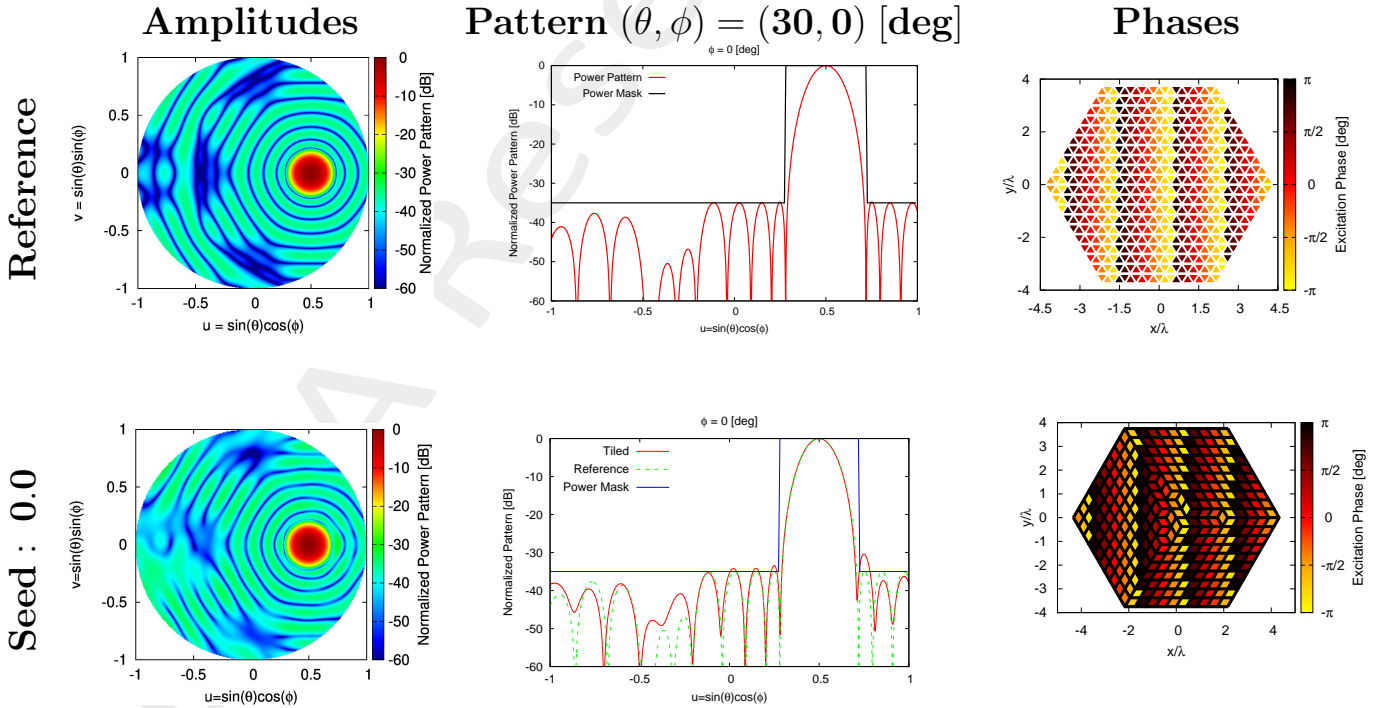


Figure 22: *Mask Matching*, $SLL = -34.79$ [dB], $N_{tot} = 600$, $L_d = 20\lambda$, $d_x = 0.22\lambda$, $d_{y1} = 0.25\lambda$, $d_{y2} = 0.5\lambda$, $a = 10$, $b = 10$, $c = 10$, $(\theta_0, \phi_0) = (30, 0)$ [deg] – Solution ID.: Reference, Seed 0.0

Solutions Summary

(a, b, c)	MAX_ITE (# iterations)	$\Delta\tau$ [sec] (single simulation period)	τ [sec] total simulation period
10, 10, 10	1000	0.091410	91.410

Table 30: Simulation Time

SOLUTION ID	SLL [dB]	HPBW (azimuth) [deg]	HPBW (elevation) [deg]	D [dB]	Mask Fitting
Reference	-34.788	10.415	8.914	26.132	0
Seed 0.0	-33.739	8.997	8.929	26.773	1.667×10^{-5}
Seed 0.15	-33.739	8.997	8.929	26.773	1.667×10^{-5}
Seed 0.205	-33.739	8.997	8.929	26.773	1.667×10^{-5}
Seed 0.222	-33.739	8.997	8.929	26.773	1.667×10^{-5}
Seed 0.283	-33.739	8.997	8.929	26.773	1.667×10^{-5}
Seed 0.440	-33.739	8.997	8.929	26.773	1.667×10^{-5}
Seed 0.441	-33.739	8.997	8.929	26.773	1.667×10^{-5}
Seed 0.45	-33.739	8.997	8.929	26.773	1.667×10^{-5}
Seed 0.597	-33.739	8.997	8.929	26.773	1.667×10^{-5}
Seed 0.649	-33.739	8.997	8.929	26.773	1.667×10^{-5}

Table 31: SLL, $HPBW_{az}$, $HPBW_{el}$, D, Mask Fitting of Radiation Pattern along $(\theta_0, \phi_0) = (30, 0)$ [deg]

1.4 OTM - Integer - Hexagon (10,10,10) - Mask Matching - Broadside - $d_{y2} = 0.5\lambda$
 - Markov Init. $N_I = 542$

Array Geometry

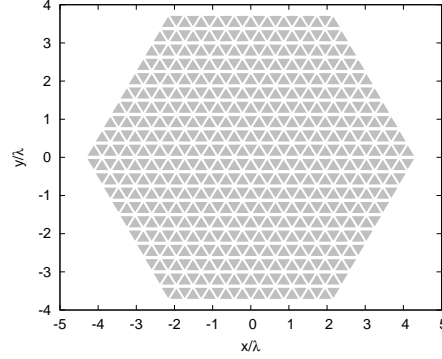


Figure 23: $N_{tot} = 600$, $L_d = 20\lambda$, $d_x = 0.22\lambda$, $d_{y1} = 0.25\lambda$, $d_{y2} = 0.5\lambda$, $N_c^{tot} = 800$, $N_p^{tot} = 441$, $N_p^{(bound)} = 61$, $a = 10$, $b = 10$, $c = 10$ – Array Geometry

Reference Array, Convex Programming Excitations

Test case parameters

- Number of array elements - $N_{tot} = 600$
- Element spacing along x - $d_x = 0.22\lambda$
- Element spacing along y_1 - $d_{y1} = 0.25\lambda$
- Element spacing along y_2 - $d_{y2} = 0.5\lambda$
- Pointing Direction - $\theta_0 = 0^\circ$
- Pointing Direction - $\phi_0 = 0^\circ$
- Pointing Direction - $u_0 = 0$
- Pointing Direction - $v_0 = 0$
- A side length - $a = 10$
- B side length - $b = 10$
- C side length - $c = 10$

Mask Constraints

The following mask (Fig.24) is used to calculate the fitness function.

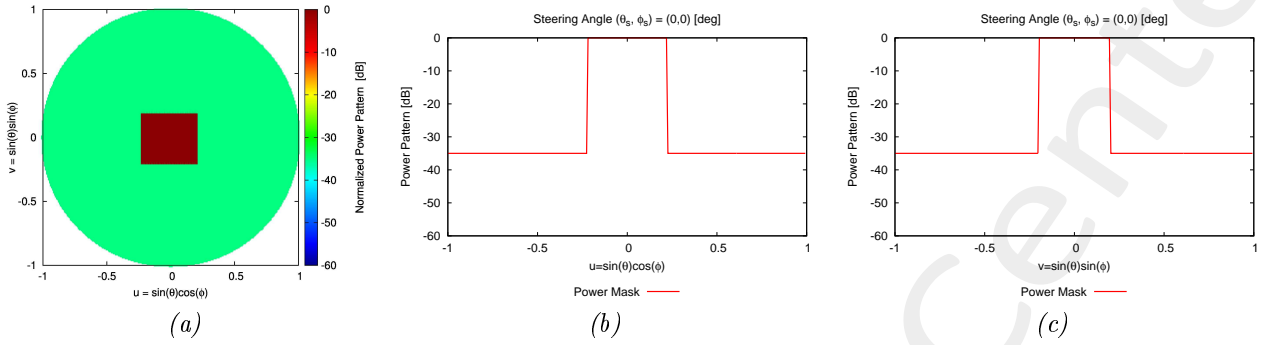


Figure 24: Mask Power Pattern in broadside direction $(\theta, \phi) = (0, 0)$ [deg]: (a) 2D, (b) Normalized cut along azimuth direction, (c) Normalized cut along elevation direction.

Best Individuals

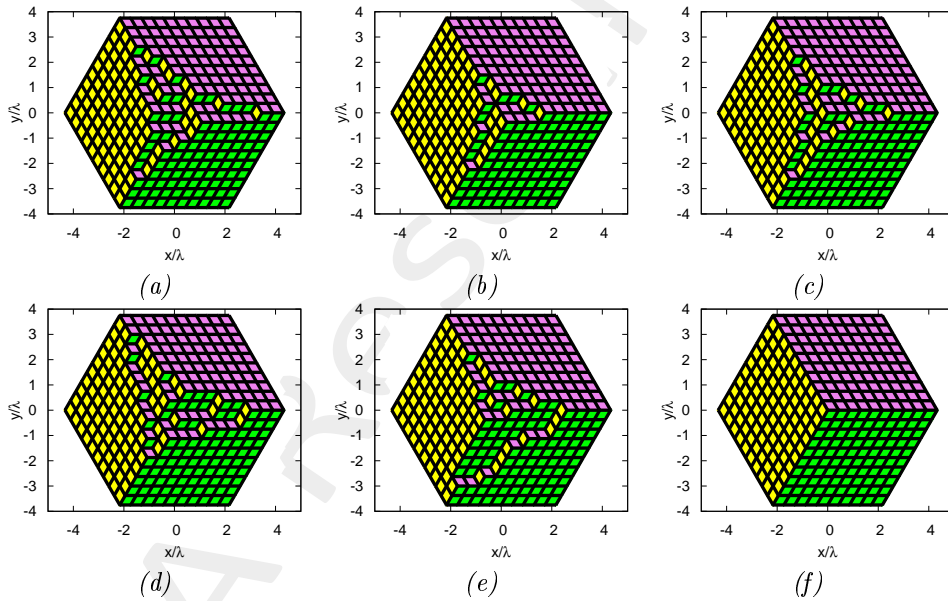


Figure 25: Best individuals of initial population: (a) Individual nr. 5, (b) Individual nr. 17, (c) Individual nr. 19, (d) Individual nr. 26, (e) Individual nr. 30, (f) Individual nr. 391.

Array Tiling

Software Parameters

The parameters are:

- Number of array elements - $N_{tot} = 600$
- Element spacing along x - $d_x = 0.22\lambda$

- Element spacing along y_1 - $d_{y1} = 0.25\lambda$
- Element spacing along y_2 - $d_{y2} = 0.5\lambda$
- Side's domain - $L_d = 20\lambda$
- Points number - $N_p^{tot} = 441$
- Points along x - $M_p = 21$
- Points along y - $N_p = 21$
- Total cells number - $N_c^{tot} = 800$
- Cells along x - $M_c = 40$
- Cells along y - $N_c = 20$
- Boundary points - $N_p^{(bound)} = 61$
- Samples along u - $N_u = 256$
- Samples along v - $N_v = 256$
- SLL weight - $w_{SLL} = 0.0$
- Directivity weight - $w_D = 0$
- HPBW weight azimuth - $w_{HPBW}^{azm} = 0.0$
- HPBW weight elevation - $w_{HPBW}^{elv} = 0.0$
- Mask weight - $w_{mask} = 1.0$
- Cell elements - $N_{el} = 1$
- Pointing Direction - $\theta_0 = 0^\circ$
- Pointing Direction - $\phi_0 = 0^\circ$
- Pointing Direction - $u_0 = 0$
- Pointing Direction - $v_0 = 0$
- A side length - $a = 10$
- B side length - $b = 10$
- C side length - $c = 10$
- A side length in λ - $L_a = 4.33\lambda$
- B side length in λ - $L_b = 4.33\lambda$

- C side length in λ - $L_c = 4.33\lambda$
- Tiling configurations - $T = 9.27 \times 10^{33}$
- Number of unknowns - $N_u = 271$
- Maximum of word max - $U_{max} = 10$
- Number of trials (seed) - $N_{seed} = 105$
- Number of individuals - $N_I = 542$
- Number of flips - $N_{flips} = 500$
- Cross-Over probability - $p_{cx} = 0.9$
- Mutation probability - $p_m = 0.001$

ELEDIA Research Center

Results

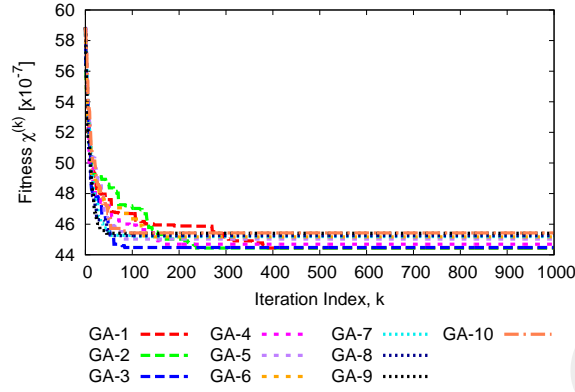


Figure 26: Fitness for 10 best seeds

GA	Seed	SLL [dB]	HPBW (az) [deg]	HPBW (el) [deg]	D [dB]	Fitness Value
1	0.1	-33.71	8.997	8.928	26.773	4.444×10^{-6}
2	0.559	-33.71	8.997	8.928	26.773	4.444×10^{-6}
3	0.441	-33.71	8.997	8.928	26.773	4.448×10^{-6}
4	0.668	-33.69	8.997	8.927	26.773	4.469×10^{-6}
5	0.65	-33.67	8.996	8.927	26.773	4.502×10^{-6}
6	0.126	-33.65	8.997	8.928	26.773	4.517×10^{-6}
7	0.903	-33.67	8.998	8.928	26.772	4.519×10^{-6}
8	0.243	-33.63	8.996	8.927	26.773	4.525×10^{-6}
9	0.511	-33.64	8.997	8.928	26.772	4.541×10^{-6}
10	0.062	-33.63	8.997	8.927	26.772	4.543×10^{-6}

Table 35: Solution Parameters of Radiation Pattern along $(\theta_0, \phi_0) = (0, 0)$ [deg]

Fig. 26 represents the fitness value for 10 best seeds.

I analyzed the solution (seed) that permits to reach the minimum fitness value. The solutions analyzed corresponds to $seed = \{0.1, 0.441, 0.559\}$.

Broadside Analysis

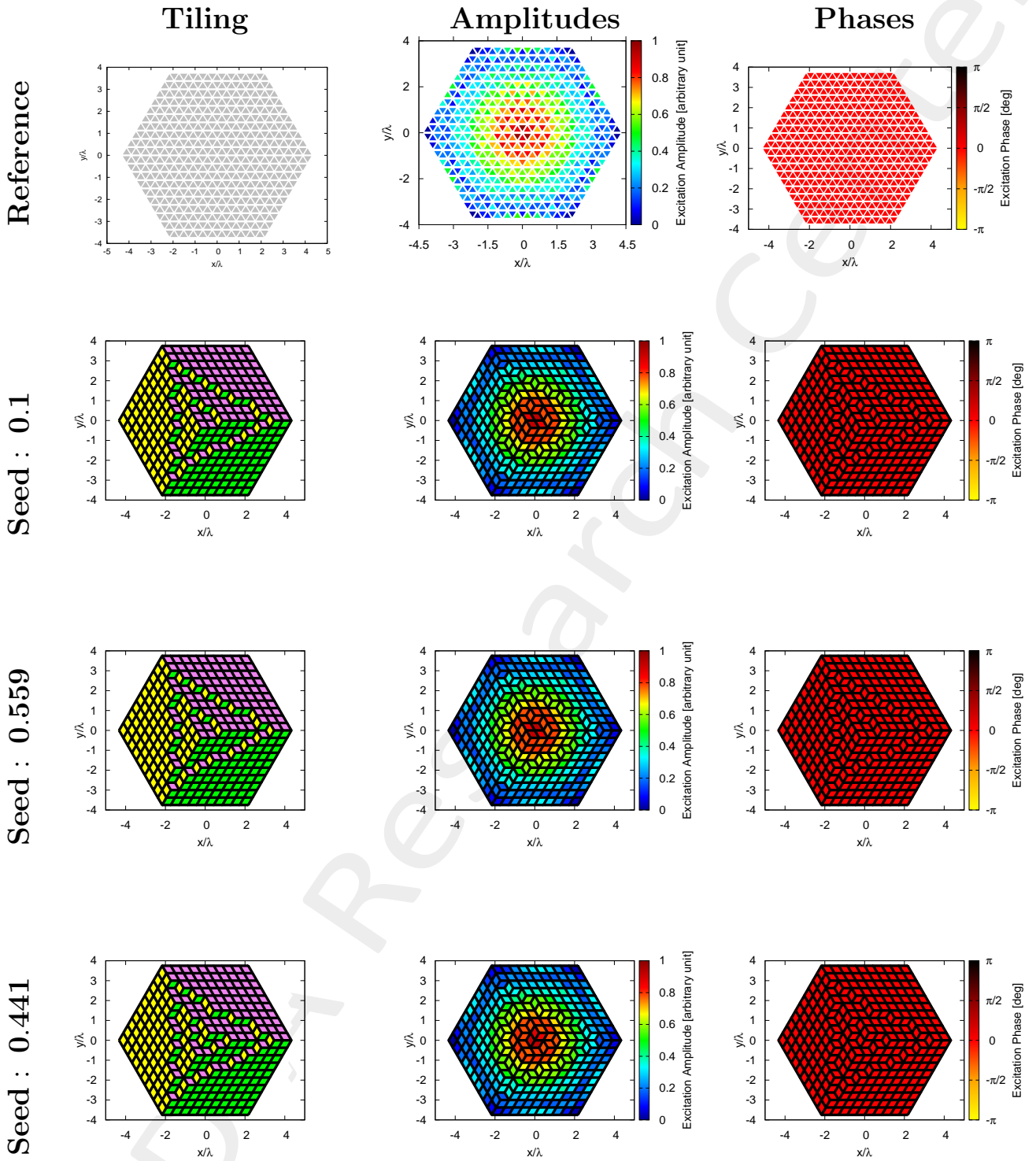


Figure 27: *Mask Matching*, $SLL = -34.79$ [dB], $N_{tot} = 600$, $L_d = 20\lambda$, $d_x = 0.22\lambda$, $d_{y1} = 0.25\lambda$, $d_{y2} = 0.5\lambda$, $a = 10$, $b = 10$, $c = 10$, $(\theta_0, \phi_0) = (0, 0)$ [deg] – Solution ID.: Reference, Seed 0.1, Seed 0.559, Seed 0.441

The best solutions have the same tiling configuration, so the radiation properties are the same, so I analyze only the solutions with $seed = \{0.0, 0.441\}$.

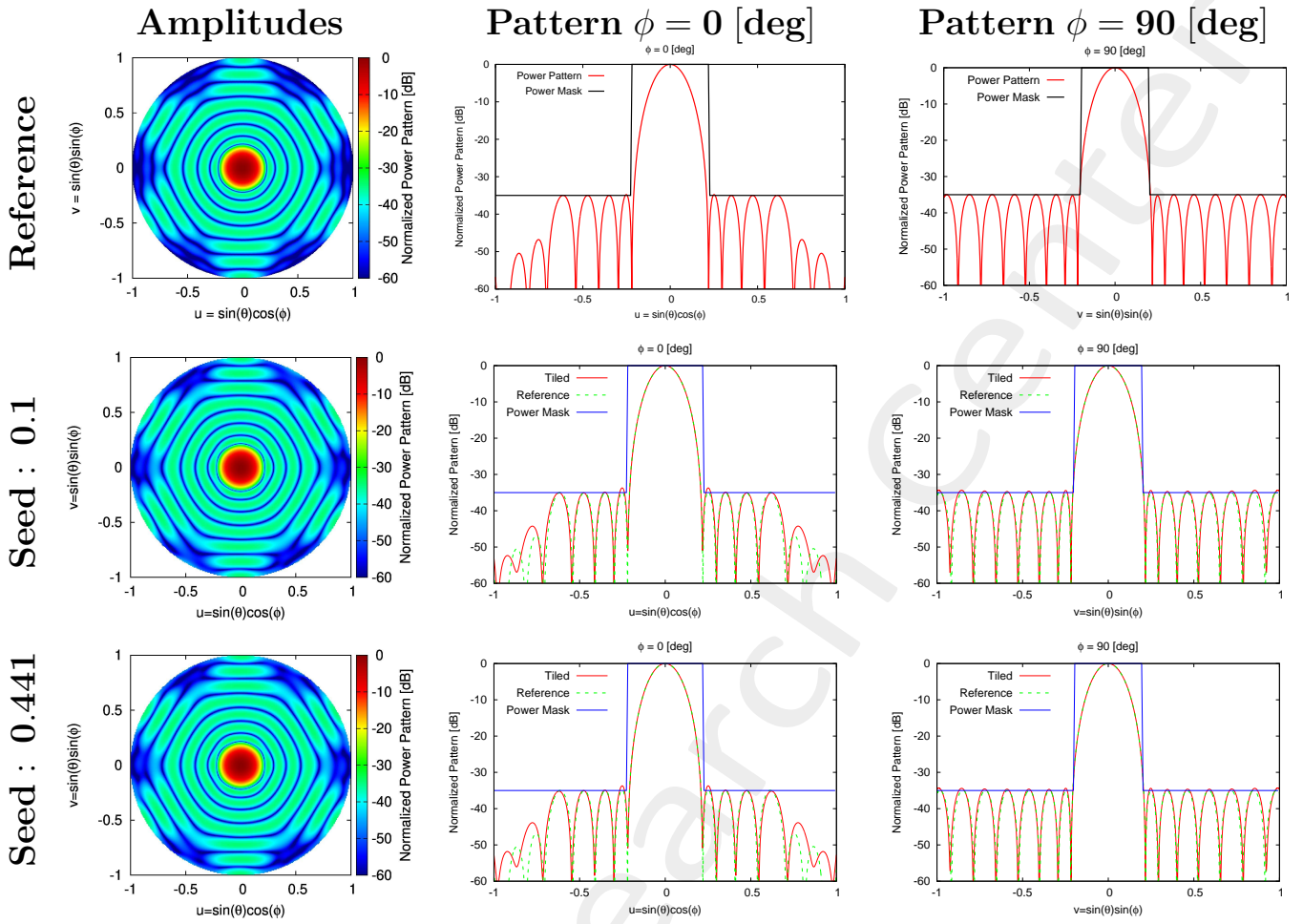


Figure 28: *Mask Matching*, $SLL = -34.79$ [dB], $N_{tot} = 600$, $L_d = 20\lambda$, $d_x = 0.22\lambda$, $d_{y1} = 0.25\lambda$, $d_{y2} = 0.5\lambda$, $a = 10$, $b = 10$, $c = 10$, $(\theta_0, \phi_0) = (0, 0)$ [deg] – Solution ID.: Reference, Seed 0.1, Seed 0.441

Steering Analysis

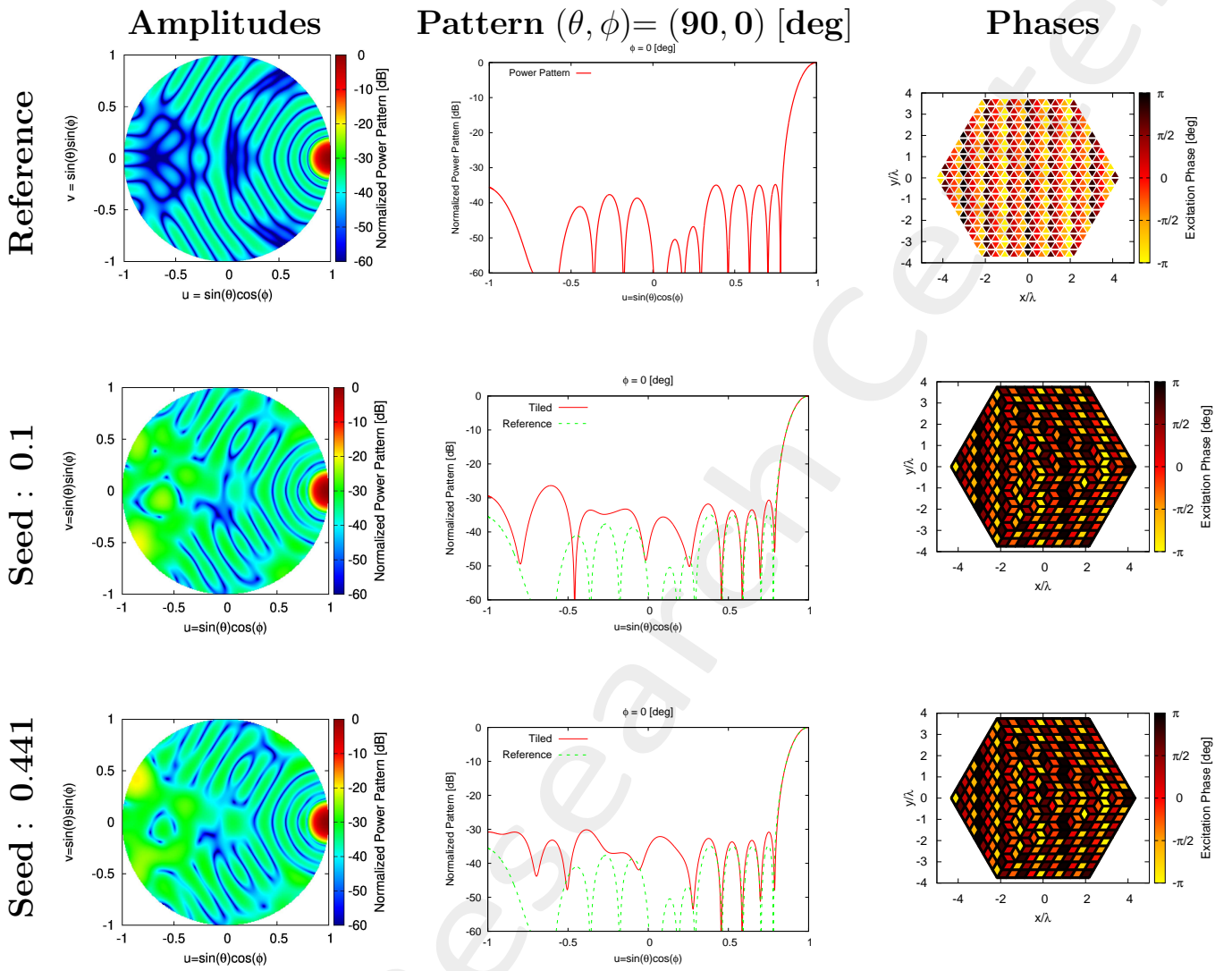


Figure 29: Mask Matching, $SLL = -34.79$ [dB], $N_{tot} = 600$, $L_d = 20\lambda$, $d_x = 0.22\lambda$, $d_{y1} = 0.25\lambda$, $d_{y2} = 0.5\lambda$, $a = 10$, $b = 10$, $c = 10$, $(\theta_0, \phi_0) = (90, 0)$ [deg] – Solution ID.: Reference, Seed 0.1, Seed 0.441

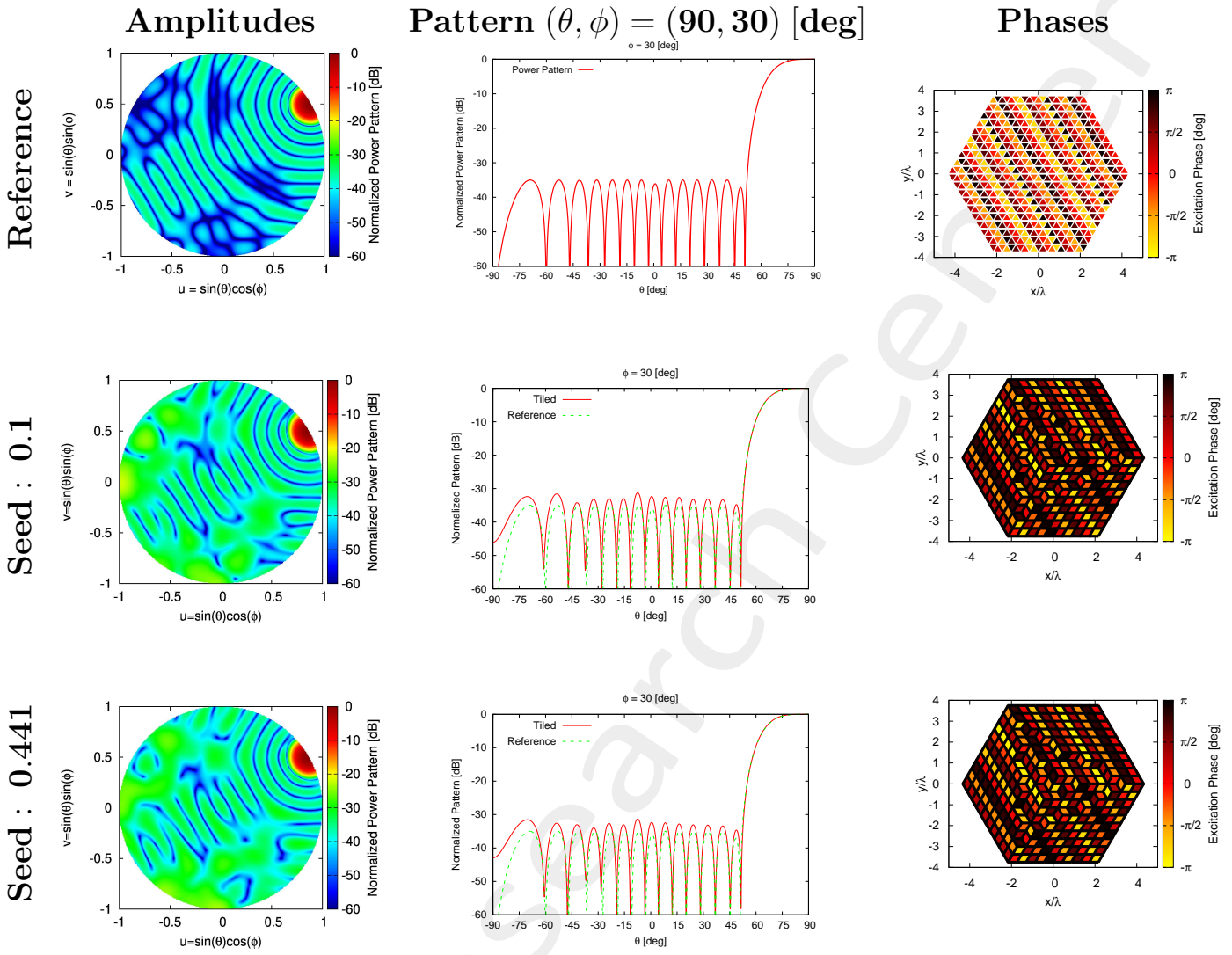


Figure 30: *Mask Matching*, $SLL = -34.79$ [dB], $N_{tot} = 600$, $L_d = 20\lambda$, $d_x = 0.22\lambda$, $d_{y1} = 0.25\lambda$, $d_{y2} = 0.5\lambda$, $a = 10$, $b = 10$, $c = 10$, $(\theta_0, \phi_0) = (90, 30)$ [deg] – Solution ID.: Reference, Seed 0.1, Seed 0.441

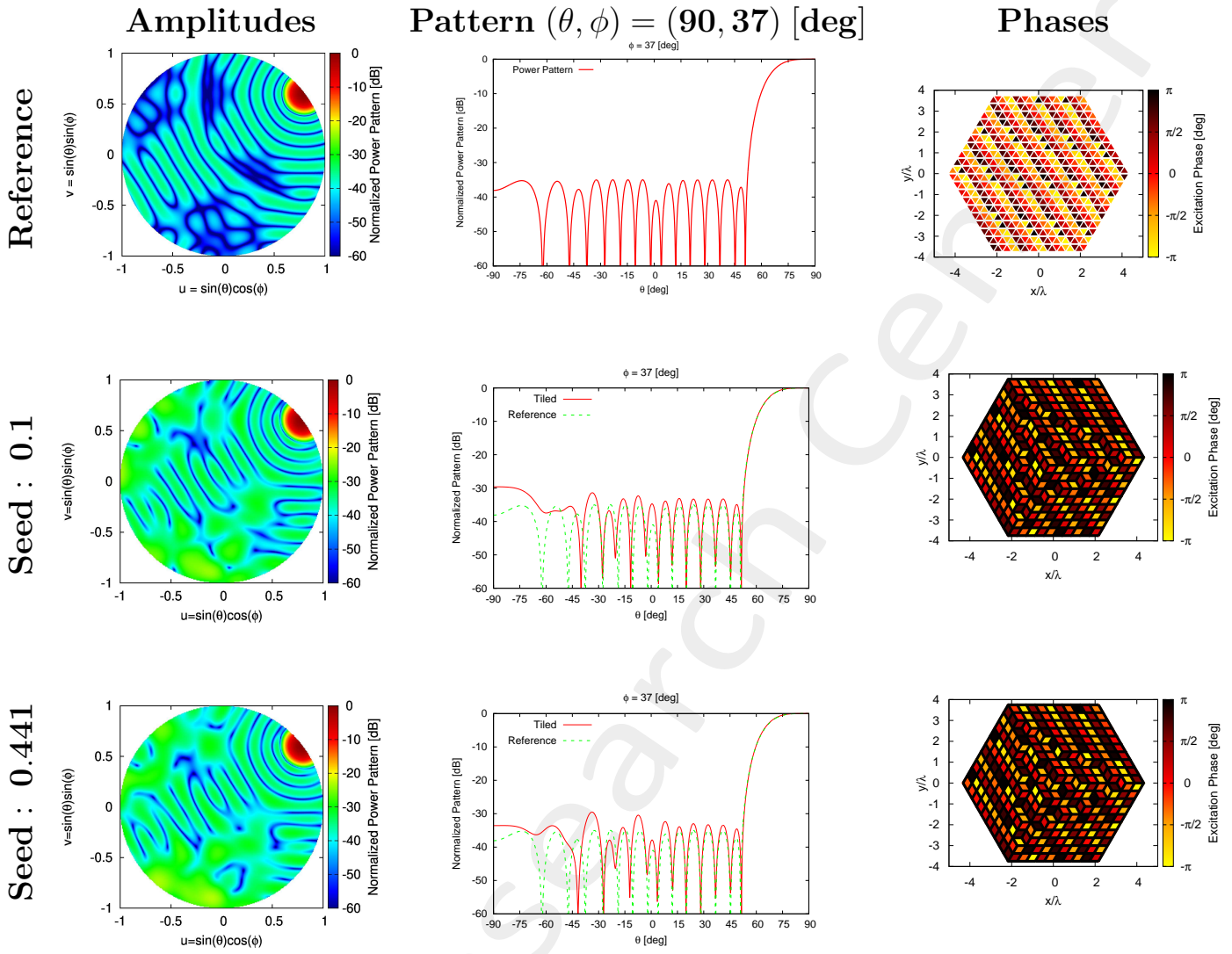


Figure 31: *Mask Matching*, $SLL = -34.79$ [dB], $N_{tot} = 600$, $L_d = 20\lambda$, $d_x = 0.22\lambda$, $d_{y1} = 0.25\lambda$, $d_{y2} = 0.5\lambda$, $a = 10$, $b = 10$, $c = 10$, $(\theta_0, \phi_0) = (90, 37)$ [deg] – Solution ID.: Reference, Seed 0.1, Seed 0.441

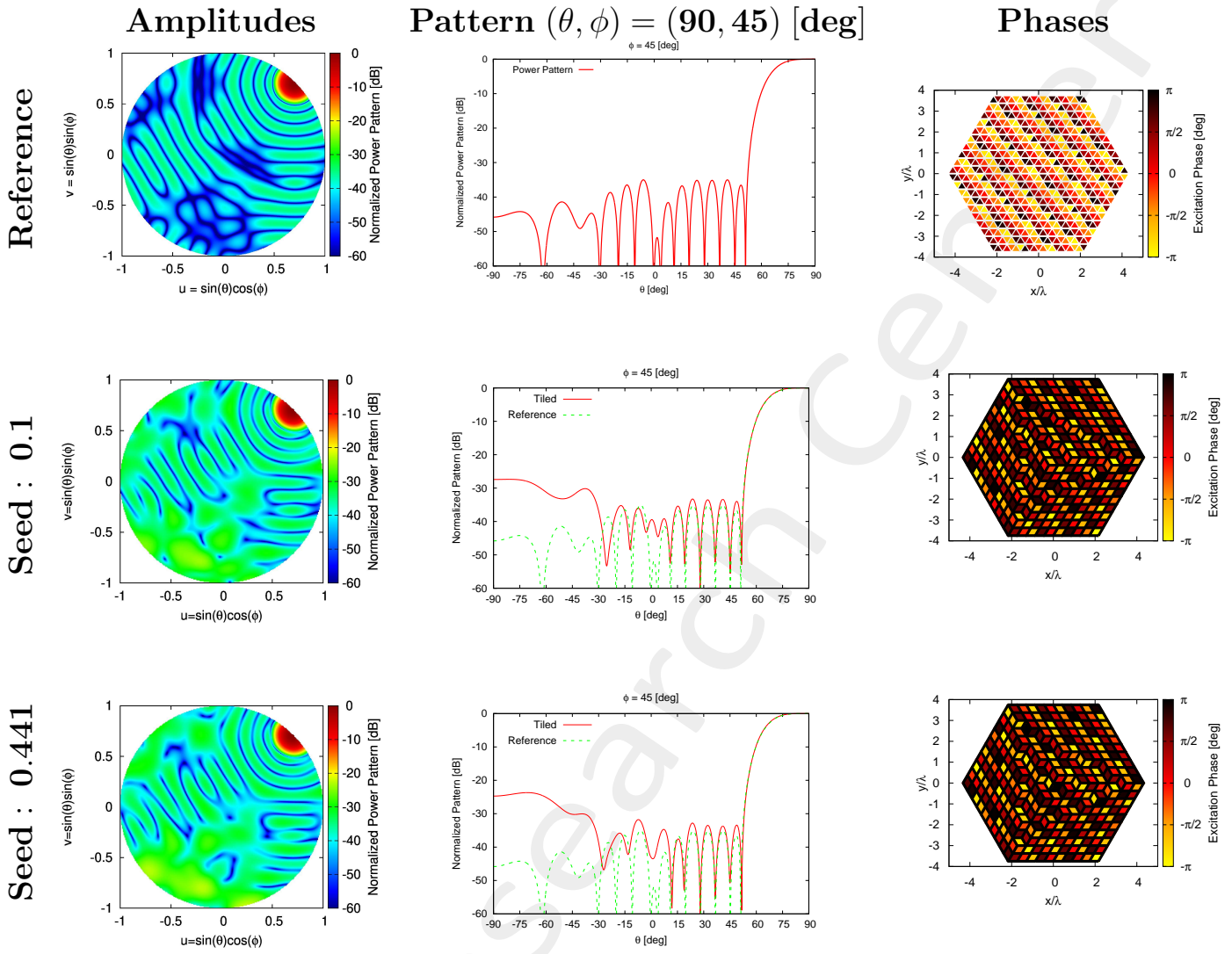


Figure 32: *Mask Matching*, $SLL = -34.79$ [dB], $N_{tot} = 600$, $L_d = 20\lambda$, $d_x = 0.22\lambda$, $d_{y1} = 0.25\lambda$, $d_{y2} = 0.5\lambda$, $a = 10$, $b = 10$, $c = 10$, $(\theta_0, \phi_0) = (90, 45)$ [deg] – Solution ID.: Reference, Seed 0.1, Seed 0.441

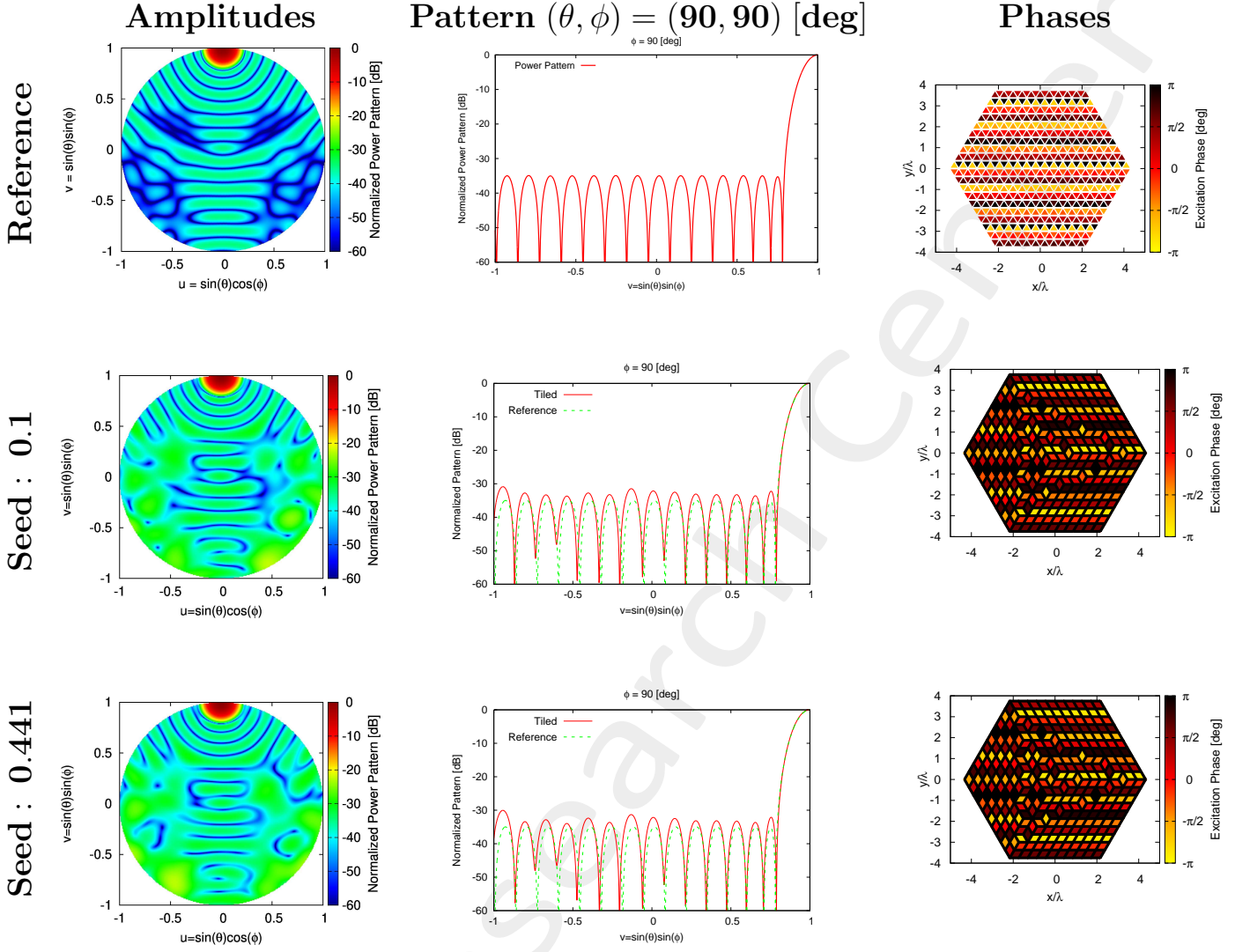


Figure 33: *Mask Matching*, $SLL = -34.79$ [dB], $N_{tot} = 600$, $L_d = 20\lambda$, $d_x = 0.22\lambda$, $d_{y1} = 0.25\lambda$, $d_{y2} = 0.5\lambda$, $a = 10$, $b = 10$, $c = 10$, $(\theta_0, \phi_0) = (90, 90)$ [deg] – Solution ID.: Reference, Seed 0.1, Seed 0.441

Solutions Summary

(a, b, c)	MAX_ITE (# iterations)	$\Delta\tau$ [sec] (single simulation period)	τ [sec] total simulation period
10, 10, 10	1000	0.216603	216.603

Table 43: Simulation Time

SOLUTION ID	SLL [dB]	HPBW (azimuth) [deg]	HPBW (elevation) [deg]	D [dB]	Mask Fitting
Reference	-34.788	9.003	8.914	26.791	0
Seed 0.1	-33.71	8.997	8.928	26.773	4.444×10^{-6}
Seed 0.559	-33.71	8.997	8.928	26.773	4.444×10^{-6}
Seed 0.441	-33.71	8.997	8.928	26.773	4.448×10^{-6}

Table 44: SLL , $HPBW_{az}$, $HPBW_{el}$, D , *Mask Fitting of Radiation Pattern* along $(\theta_0, \phi_0) = (0, 0)$ [deg]

More information on the topics of this document can be found in the following list of references.

References

- [1] P. Rocca, M. Benedetti, M. Donelli, D. Franceschini, and A. Massa, "Evolutionary optimization as applied to inverse problems," *Inverse Problems - 25 th Year Special Issue of Inverse Problems, Invited Topical Review*, vol. 25, pp. 1-41, Dec. 2009
- [2] P. Rocca, G. Oliveri, and A. Massa, "Differential Evolution as applied to electromagnetics," *IEEE Antennas Propag. Mag.*, vol. 53, no. 1, pp. 38-49, Feb. 2011
- [3] P. Rocca, N. Anselmi, A. Polo, and A. Massa, "An irregular two-sizes square tiling method for the design of isophoric phased arrays," *IEEE Trans. Antennas Propag.*, vol. 68, no. 6, pp. 4437-4449, Jun. 2020
- [4] P. Rocca, N. Anselmi, A. Polo, and A. Massa, "Modular design of hexagonal phased arrays through diamond tiles," *IEEE Trans. Antennas Propag.*, vol.68, no. 5, pp. 3598-3612, May 2020
- [5] N. Anselmi, L. Poli, P. Rocca, and A. Massa, "Design of simplified array layouts for preliminary experimental testing and validation of large AESAs," *IEEE Trans. Antennas Propag.*, vol. 66, no. 12, pp. 6906-6920, Dec. 2018
- [6] N. Anselmi, P. Rocca, M. Salucci, and A. Massa, "Contiguous phase-clustering in multibeam-on-receive scanning arrays," *IEEE Trans. Antennas Propag.*, vol. 66, no. 11, pp. 5879-5891, Nov. 2018
- [7] G. Oliveri, G. Gottardi, F. Robol, A. Polo, L. Poli, M. Salucci, M. Chuan, C. Massagrande, P. Vinetti, M. Mattivi, R. Lombardi, and A. Massa, "Co-design of unconventional array architectures and antenna elements for 5G base station," *IEEE Trans. Antennas Propag.*, vol. 65, no. 12, pp. 6752-6767, Dec. 2017
- [8] N. Anselmi, P. Rocca, M. Salucci, and A. Massa, "Irregular phased array tiling by means of analytic schemata-driven optimization," *IEEE Trans. Antennas Propag.*, vol. 65, no. 9, pp. 4495-4510, September 2017
- [9] N. Anselmi, P. Rocca, M. Salucci, and A. Massa, "Optimization of excitation tolerances for robust beam-forming in linear arrays," *IET Microwaves, Antennas & Propagation*, vol. 10, no. 2, pp. 208-214, 2016
- [10] P. Rocca, R. J. Mailloux, and G. Toso, "GA-Based optimization of irregular sub-array layouts for wideband phased arrays desig," *IEEE Antennas and Wireless Propag. Lett.*, vol. 14, pp. 131-134, 2015
- [11] P. Rocca, M. Donelli, G. Oliveri, F. Viani, and A. Massa, "Reconfigurable sum-difference pattern by means of parasitic elements for forward-looking monopulse radar," *IET Radar, Sonar & Navigation*, vol 7, no. 7, pp. 747-754, 2013
- [12] P. Rocca, L. Manica, and A. Massa, "Ant colony based hybrid approach for optimal compromise sum-difference patterns synthesis," *Microwave Opt. Technol. Lett.*, vol. 52, no. 1, pp. 128-132, Jan. 2010

- [13] P. Rocca, L. Manica, and A. Massa, "An improved excitation matching method based on an ant colony optimization for suboptimal-free clustering in sum-difference compromise synthesis," *IEEE Trans. Antennas Propag.*, vol. 57, no. 8, pp. 2297-2306, Aug. 2009
- [14] M. Salucci, L. Poli, A. F. Morabito, and P. Rocca, "Adaptive nulling through subarray switching in planar antenna arrays," *Journal of Electromagnetic Waves and Applications*, vol. 30, no. 3, pp. 404-414, February 2016
- [15] T. Moriyama, L. Poli, and P. Rocca, "Adaptive nulling in thinned planar arrays through genetic algorithms," *IEICE Electronics Express*, vol. 11, no. 21, pp. 1-9, Sep. 2014
- [16] L. Poli, P. Rocca, M. Salucci, and A. Massa, "Reconfigurable thinning for the adaptive control of linear arrays," *IEEE Trans. Antennas Propag.*, vol. 61, no. 10, pp. 5068-5077, Oct. 2013
- [17] P. Rocca, L. Poli, G. Oliveri, and A. Massa, "Adaptive nulling in time-varying scenarios through time-modulated linear arrays," *IEEE Antennas Wireless Propag. Lett.*, vol. 11, pp. 101-104, 2012
- [18] M. Benedetti, G. Oliveri, P. Rocca, and A. Massa, "A fully-adaptive smart antenna prototype: ideal model and experimental validation in complex interference scenarios," *Progress in Electromagnetic Research, PIER* 96, pp. 173-191, 2009
- [19] P. Rocca, L. Poli, A. Polo, and A. Massa, "Optimal excitation matching strategy for sub-arrayed phased linear arrays generating arbitrary shaped beams," *IEEE Trans. Antennas Propag.*, vol. 68, no. 6, pp. 4638-4647, Jun. 2020
- [20] G. Oliveri, G. Gottardi and A. Massa, "A new meta-paradigm for the synthesis of antenna arrays for future wireless communications," *IEEE Trans. Antennas Propag.*, vol. 67, no. 6, pp. 3774-3788, Jun. 2019
- [21] P. Rocca, M. H. Hannan, L. Poli, N. Anselmi, and A. Massa, "Optimal phase-matching strategy for beam scanning of sub-arrayed phased arrays," *IEEE Trans. Antennas and Propag.*, vol. 67, no. 2, pp. 951-959, Feb. 2019
- [22] L. Poli, G. Oliveri, P. Rocca, M. Salucci, and A. Massa, "Long-Distance WPT Unconventional Arrays Synthesis," *Journal of Electromagnetic Waves and Applications*, vol. 31, no. 14, pp. 1399-1420, Jul. 2017
- [23] G. Gottardi, L. Poli, P. Rocca, A. Montanari, A. Aprile, and A. Massa, "Optimal Monopulse Beamforming for Side-Looking Airborne Radars," *IEEE Antennas Wireless Propag. Lett.*, vol. 16, pp. 1221-1224, 2017
- [24] G. Oliveri, M. Salucci, and A. Massa, "Synthesis of modular contiguously clustered linear arrays through a sparseness-regularized solver," *IEEE Trans. Antennas Propag.*, vol. 64, no. 10, pp. 4277-4287, Oct. 2016
- [25] P. Rocca, G. Oliveri, R. J. Mailloux, and A. Massa, "Unconventional phased array architectures and design Methodologies - A review," *Proceedings of the IEEE = Special Issue on 'Phased Array Technologies', Invited Paper*, vol. 104, no. 3, pp. 544-560, March 2016

- [26] P. Rocca, M. D'Urso, and L. Poli, "Advanced strategy for large antenna array design with subarray-only amplitude and phase contr," *IEEE Antennas and Wireless Propag. Lett.*, vol. 13, pp. 91-94, 2014
- [27] L. Manica, P. Rocca, G. Oliveri, and A. Massa, "Synthesis of multi-beam sub-arrayed antennas through an excitation matching strategy," *IEEE Trans. Antennas Propag.*, vol. 59, no. 2, pp. 482-492, Feb. 2011
- [28] G. Oliveri, "Multi-beam antenna arrays with common sub-array layouts," *IEEE Antennas Wireless Propag. Lett.*, vol. 9, pp. 1190-1193, 2010
- [29] P. Rocca, R. Haupt, and A. Massa, "Sidelobe reduction through element phase control in sub-arrayed array antennas," *IEEE Antennas Wireless Propag. Lett.*, vol. 8, pp. 437-440, 2009
- [30] P. Rocca, L. Manica, R. Azaro, and A. Massa, "A hybrid approach for the synthesis of sub-arrayed monopulse linear arrays," *IEEE Trans. Antennas Propag.*, vol. 57, no. 1, pp. 280-283, Jan. 2009
- [31] L. Manica, P. Rocca, M. Benedetti, and A. Massa, "A fast graph-searching algorithm enabling the efficient synthesis of sub-arrayed planar monopulse antennas," *IEEE Trans. Antennas Propag.*, vol. 57, no. 3, pp. 652-664, Mar. 2009
- [32] P. Rocca, L. Manica, A. Martini, and A. Massa, "Compromise sum-difference optimization through the iterative contiguous partition method," *IET Microwaves, Antennas & Propagation*, vol. 3, no. 2, pp. 348-361, 2009
- [33] L. Manica, P. Rocca, and A. Massa, "An excitation matching procedure for sub-arrayed monopulse arrays with maximum directivity," *IET Radar, Sonar & Navigation*, vol. 3, no. 1, pp. 42-48, Feb. 2009
- [34] L. Manica, P. Rocca, and A. Massa, "Design of subarrayed linear and planar array antennas with SLL control based on an excitation matching approach," *IEEE Trans. Antennas Propag.*, vol. 57, no. 6, pp. 1684-1691, Jun. 2009